Anal Bioanal Chem (2010) 398:613–650
DOI 10.1007/s00216-010-3881-7

REVIEW

Mechanisms and measurements of nanomaterial-induced oxidative damage to DNA

Elijah J. Petersen · Bryant C. Nelson

Received: 5 March 2010 / Revised: 24 May 2010 / Accepted: 26 May 2010 / Published online: 22 June 2010

Abstract Many of the current investigations on the environmental and human health risks of engineered nanomaterials focus on their short-term acute toxicity. However, the long-term chronic effects of nanomaterials on living systems, and in particular, on the genetic components of living systems, also warrant attention. An increasing number of nanomaterial safety studies include an assessment of genotoxicity as part of the overall risk evaluation. The potential of nanomaterials to directly or indirectly promote the formation of reactive oxygen species is one of the primary steps in their genotoxic repertoire. The subsequent modification of genomic DNA by reactive oxygen species could lead to the development of mutagenesis, carcinogenesis, or other age-related diseases if the DNA damage is not repaired. This review focuses on the interactions of nanomaterials with DNA and specifically on the capacity of some nanomaterials to induce oxidative damage to DNA. A critical assessment of the analytical methodology and the potential biochemical mechanisms involved in nanomaterial induction of oxidative damage to DNA is presented, results obtained for the various studies with each nanomaterial are compared, and recommendations for future research are discussed. Researchers should consider, among other experimental recommendations, (1) the application of more chromatography-based and mass-spectrometry-based analytical techniques to the assessment of oxidative damage to DNA to facilitate an enhanced understanding of DNA damage mechanisms and (2) the verification of cellular viability before conducting genotoxicity assays to reduce the impact of fragmented DNA, formed as a consequence of cell death, on DNA damage measurements.

Keywords Base lesions · Comet assay · DNA damage · Engineered nanomaterials · Genotoxicity · Toxicity

Introduction

Engineered or manufactured nanomaterials (ENs) are particles, fibers, tubes, spheres, rods, etc., of varied compositions that contain at least one dimension that measures 100 nm or less [1]. Partly because of their reduced sizes and larger surface area to volume ratios in comparison with microscale or macroscale materials of identical composition, ENs are typically highly surface reactive (i.e., catalytic) and show enhanced physical (i.e., higher tensile strength), chemical (i.e., persistent redox cycling) and electronic (i.e., semiconducting) properties [2, 3]. Thus, there is strong scientific and commercial interest in the development and use of ENs in fields such as engineering, agriculture, electronics, and medicine. Research- and industrial-scale developments of ENs are already proceeding at a rapid pace, with many consumer products such as athletic equipment (e.g., tennis racquets), cosmetics (e.g., suntan lotions), and laundry products (e.g., fabric softeners) already containing significant amounts of ENs (for the full list of consumer products containing ENs, it is suggested that the reader visit the following Web site: http://www.nanotechproject.org/inventories/consumer/). The critical problem is that the understanding of the

Electronic supplementary material The online version of this article (doi:10.1007/s00216-010-3881-7) contains supplementary material, which is available to authorized users.

E. J. Petersen · B. C. Nelson (✉)
Chemical Science and Technology Laboratory, Biochemical Science Division, National Institute of Standards and Technology, 100 Bureau Drive, Stop 8311, Gaithersburg, MD 20899-0001, USA
e-mail: bryant.nelson@nist.gov

environmental health and human safety risks of ENs has lagged behind their incorporation in commercial goods. In our opinion, comprehensive in vitro (acellular and cellular) and in vivo toxicity studies using appropriate models (cells, organisms, animals, plants) are needed to evaluate the acute and chronic biological effects of ENs that could potentially lead to toxicity. Most of the current studies utilize in vitro models and focus primarily on toxicity end points dealing with cellular viability, i.e., apoptosis, necrosis, etc. These types of studies are definitely needed, but there is a growing consensus that complementary studies are needed that focus on the chronic biological effects of ENs such as their potential genotoxicity [4–6].

Understanding the long-term interactions of ENs with DNA and the mechanisms of those interactions is important for evaluating and predicting mutation- and cancer-related risks of ENs. Traditional genotoxic end points such as gene mutations (assessed via the Ames *Salmonella* test or the hypoxanthine phosphoribosyltransferase forward mutation assay), chromosomal damage (assessed via the micronuclease test), and oxidative damage to DNA [assessed via the single cell gel electrophoresis (comet) assay] have been utilized with increasing frequency for the evaluation of EN-induced genotoxicity.

EN-induced oxidative stress is perhaps the most broadly developed and accepted mechanism for the potential toxic activity of ENs [1]. There are three main hypothetical scenarios whereby ENs might induce oxidative stress and the subsequent generation of excess intra- and extracellular reactive oxygen species (ROS) and, to a lesser extent, reactive nitrogen species that have the capacity to overwhelm a biological system's (cell, organism, plant, animal, etc.) natural antioxidant defense mechanisms [7]. First, the ENs might be inherently redox-active or have surface features/properties that catalyze redox activity, leading to oxidative stress and to generation of excess ROS. Second, the ENs might be biopersistent, meaning that once ENs enter a biological system, they do not degrade or break down over time but instead remain in the system, inducing site-specific and possibly systemic inflammation. Inflammation initiates the recruitment of inflammatory leukocytes (monocytes, neutrophils, etc.), which then become activated and generate excess ROS [8]. Third, the ENs might enter the cell and physically interact with and structurally damage subcellular organelles such as mitochondria. In such cases, the damaged mitochondria could lead to disruption of the electron transport chain and the production of adenosine triphosphate (ATP), which could again lead to the generation of excess ROS. Many ENs have already demonstrated the ability to directly or indirectly induce the formation of ROS in in vitro and in vivo studies [1]. The generated ROS, especially the extremely reactive hydroxyl radical (•OH), have the capability to attack DNA via several different mechanisms to generate single-strand breaks (SSBs), double-strand breaks (DSBs), oxidatively induced base damage, and other DNA lesions [9]. The accumulation of SSBs and oxidatively induced base lesions can lead to DSBs, considered the most lethal type of oxidative damage to DNA [10]. Compared with other types of DNA damage, DSBs are intrinsically more difficult to repair and as little as one DSB lesion in a cell can kill the cell if the lesion inactivates a critical gene [10]. SSB and oxidatively induced DNA base lesions are definitely not harmless, and are known to block DNA transcription and replication processes, resulting in accelerated cytotoxicity and genomic instability [9, 11].

For the specific case of EN-induced oxidative damage to DNA, the comet assay [12–15] is the most widely utilized method for evaluating the extent of genomic DNA damage (see Table 1). The principle of the assay is simple—individual cells are lysed and the DNA is subjected to agarose gel electrophoresis under either alkaline or neutral conditions, depending on whether one wants to detect predominantly SSBs or predominantly DSBs, respectively. The DNA is then stained using a fluorescent, intercalating dye such as ethidium bromide and the image (a comet) that is formed comprises intact DNA and a tail consisting of damaged DNA strands (see Fig. 1). The comet images are compared against controls to determine the number of DNA strand breaks; larger comets are correlated with the presence of more extensive strand breaks. The alkaline comet assay can also be modified to specifically detect the occurrence of oxidized purine base lesions and/or oxidized pyrimidine base lesions through the incorporation of either purine-specific [*Escherichia coli* formamidopyrimidine glycosylase (Fpg)] or pyrimidine-specific [(*E. coli* endonuclease III (Nth)] base excision repair (BER) enzymes in the assay protocol. These enzymes will remove the base lesion and then generate a DNA strand break at the abasic site that can be detected via the comet assay. The use of BER enzymes in the comet assay allows one to estimate the relative level of oxidatively induced DNA base damage, but does not allow identification of the specific modified DNA base nor absolute quantification of the damage. Additionally, the alkaline comet assay can be used to detect alkali-labile sites (ALS), which are sites of oxidative damage that can be converted to strand breaks through the use of alkaline denaturing conditions in the assay protocol. ALS include both apurinic and apyrimdinic sites that are formed owing to BER processes. A problem that makes comparing comet assay results between or among laboratories difficult is that the different types of DNA damage are often reported in arbitrary comet score units (i.e., percentage DNA in tail, tail moment, etc.) that are not traceable to any standard. Recently, however, it was shown that the comet assay could be calibrated through the use of ionizing

radiation [16, 17]. The calibration procedure allows the comet score to be converted to equivalent radiation (Gy) units and for the subsequent calculation of the number of lesions per cell or the number of lesions per 10^6 base pairs. This development not only facilitates comparison of comet assay results between laboratories, but also has the potential to reduce assay result variability [16].

Regarding the present review, several pertinent points need to be recognized. First, it is well established that the alkaline and neutral versions of the comet assay do not solely measure SSBs and DSBs, respectively [12–15]. The alkaline comet assay measures both SSBs and DSBs, but predominantly SSBs. The neutral comet assay can be specially designed to measure solely DSBs [12], but although it typically measures both SSBs and DSBs, DSBs are predominately measured. Some studies that utilized the alkaline comet assay specifically reported the detection of oxidative damage to DNA damage as SSBs, whereas other studies only reported the DNA damage as strand breaks. For the purpose of this review and to avoid confusion during the assay assessments, when studies have utilized the alkaline comet assay, we considered the detected strand breaks to be predominantly due to SSBs with the recognition that the strand breaks are likely to be a mixture of SSBs and DSBs. We took a similar approach with the single study that utilized the neutral comet assay by reporting the strand breaks as DSBs [18]. Second, a number of studies reported the detection of strand breaks using the Fpg-modified comet assay. Many of these studies reported and plotted the resulting oxidative damage to DNA with no measurement correction, when, in fact, the true DNA damage is obtained by subtracting the strand break levels measured with the Fpg-modified assay from the strand break levels measured with the unmodified alkaline comet assay [16]. This adjustment was made in some of the studies on the effects of ENs [19–23].

Other assays that have been reported for the detection of EN-induced oxidative damage to DNA in the form of DNA strand breaks include (1) γ-H2AX assay, (2) plasmid nicking/agarose gel electrophoresis assay, and (3) alkaline precipitation assay. The γ-H2AX assay is strictly used for detection of DSBs and is based on the consensus phosphorylation of Ser-139 of the H2AX protein (a member of the H2 histone family) that occurs rapidly due to the presence of DSBs [24, 25]. The phosphorylated H2AX protein (γ-H2AX) is detected using antibodies against γ-H2AX with either immunostaining or flow cytometry (see Fig. 2). A modified version of the plasmid nicking/agarose gel electrophoresis assay [26] is also utilized to detect SSBs and DSBs induced by the nicking action of ENs on the DNA backbone. This assay is based on the conversion of supercoiled (S) plasmid DNA to either a relaxed (R) or a linear (L) form. The forms are separated using a gel-electrophoretic platform containing an intercalating fluorescent dye; the forms are separated on the basis of the differential electrophoretic mobilities among the S (migrates the fastest), L (migrates between S and R), and R (migrates the slowest) forms. Detection of the R form is indicative of SSBs and detection of the L form is indicative of DSBs. The alkaline precipitation assay [27, 28] is a rapid procedure that gives a measure of total SSBs and DSBs combined. In this procedure, cells are lysed with sodium dodecyl sulfate and the DNA and proteins are precipitated with potassium chloride. The DNA that is damaged remains in solution and therefore by taking the ratio of the amount of precipitated DNA to the amount of DNA in solution, one can roughly estimate the fraction of strand breaks.

Assays currently utilized for evaluating EN-induced oxidative damage to DNA in the form of DNA base lesions (excluding the previously described Fpg-modified comet assay) include (1) direct antibody assays for 8-hydroxy-2′-deoxyguanosine (8-OH-dG) and (2) liquid chromatography (LC) coupled with ultraviolet (UV) detection or LC with both UV and electrochemical (EC) detection for the determination of 8-OH-dG. The modified nucleoside, 8-OH-dG, is one of the most widely recognized and utilized biomarkers of oxidative stress and oxidatively induced DNA damage [29]. Many different types of biological compounds, chemical agents, and ionizing radiation have been shown to produce ROS (usually •OH) that preferentially attack guanine residues (the most easily oxidizable base) in DNA to induce the formation of 8-OH-dG as well as other modified bases [9]. There are several studies describing the use of monoclonal antibodies against 8-OH-dG, along with secondary labeled antibodies, for the evaluation of 8-OH-dG levels induced by ENs. Under this format, most studies utilize enzyme-linked immunosorbent assay (ELISA) [30] or immunohistochemical assay platforms [31] for 8-OH-dG detection and quantification. The most specific methods for the measurement of 8-OH-dG involve the use of either LC/UV or LC/UV/EC methods [32] for the selective separation and specific detection of 8-OH-dG in extracted DNA samples. In these procedures, DNA extracted from either in vitro or in vivo samples is enzymatically hydrolyzed to 2′-deoxynucleosides; 8-OH-dG, in the midst of other modified and nonmodified 2′-deoxynucleosides, is detected on the basis of either its UV absorbance or its EC oxidation properties.

In our laboratory, we employ gas chromatography/mass spectrometry (GC/MS) and liquid chromatography/tandem mass spectrometry with stable isotope-dilution procedures for detecting and quantifying oxidatively induced DNA base damage mediated through the interactions of ENs with cells and organisms. The use of isotope-dilution mass spectrometry allows us to simultaneously identify and quantify multiple (more than 20) [29] oxidatively induced

Table 1 Summary of nanomaterial-induced oxidative damage to DNA studies

Reference	Nanoparticle tested (size)	Cell/organism tested	DNA damage assay	Concentrations	Exposure duration (h)	Findings
Carbon nanoparticles						
Carbon Black						
Gallagher et al. [50]	Degussa Printex 90 (nominal size 16 nm by manufacturer) and Sterling V (particle size 70 nm by manufacturer)	Fischer 344 rats (lungs tested) by inhalation	8-OH-dG using LC/UV/EC	1.2, 7.1, and 52.8 mg/m^3 (Printex 90) or 48.2 mg/m^3 (Sterling V)	13 weeks (some organisms also had additional 44 weeks recovery)	Only 52.8 mg/m^3 of Printex 90 caused significantly elevated levels after 13 weeks of exposure After 44 weeks of recovery, only 7.1 and 52.8 mg/m^3 caused significantly elevated 8-OH-dG levels
Gerloff et al. [44]	Degussa Printex 90 (nominal size 14 nm by manufacturer)	Human carcinoma intestinal cells (Caco-2 cells)	Alkaline comet assay +/- FPG	133.3 μg/mL	4	No significant effect with or without FPG
Jacobsen et al. [21]	Degussa Printex 90 (nominal size 14 nm by manufacturer)	Fe1 Muta Mouse lung epithelial cell line	Alkaline comet assay +/- FPG	75 μg/mL	3	Significant increases observed with and without FPG
Jacobsen et al. [48]	Degussa Printex 90 (nominal size 14 nm by manufacturer)	ApoE-/- mice (bronchoalveolar lavage fluid cells tested) by intratrachael instillation	Alkaline comet assay	54 μg	3	Significant increase observed
Karlsson et al. [22]	Sigma-Aldrich carbon powder (<30 nm by manufacturer)	Human lung epithelial cell line (A549)	Alkaline comet assay +/- FPG	2, 40, and 80 μg/mL (40 and 80 μg/mL for FPG)	4	No significant increase in DNA or oxidatively modified lesions at any concentration
Mroz et al. [45]	Degussa Printex 90 (nominal size 14 nm by manufacturer) tested with and without benzo[*a*]pyrene and Huber 990 coarse carbon black (260 nm by manufacturer)	Human lung epithelial cell line (A549)	Alkaline comet assay	100 μg/mL	3	Significant increase for nanoparticulate carbon black with and without benzo[*a*]pyrene but not coarse carbon black
Mroz et al. [18]	Degussa Printex 90 (nominal size 14 nm by manufacturer) tested with and without benzo[*a*]pyrene and Huber 990 coarse carbon black (260 nm by manufacturer)	Human lung epithelial cell line (A549)	Alkaline and neutral comet assay	100 μg/mL	3	Significant increase for nanoparticulate carbon black with and without benzo[*a*]pyrene but not coarse carbon black for alkaline comet assay No significant increase for coarse or nanoparticulate carbon black with neutral comet assay
Totsuka et al. [49]	Degussa Printex 90 (nominal size 14 nm by manufacturer)	Male C57BL/6 J mice (lungs tested) by intratrachael instillation	Alkaline comet assay	0.05 and 0.2 mg per animal	3, 24	For 3 h, there was a significant increase for 0.2 mg but not 0.05 mg No change for 24 h compared with 3 h

Yang et al. [46]	Nano-Innovation (12.3± 4.1 nm, >99.4% carbon purity)	Primary mouse embryo fibroblasts	Alkaline comet assay	5 and 10 μg/mL	24	Significant effects at both concentrations
Zhong et al. [47]	Cabat carbon black (37-nm primary particle size by manufacturer)	Chinese hamster lung fibroblasts (V79 cells) and human embryonic lung fibroblasts (Hel 299 cells)	Alkaline comet assay	98, 196, 392, and 786 μg/mL	3	No effects observed with either cell at any concentration
Carbon nanofibers						
Lindberg et al. [52]	Sigma-Aldrich graphitic nanofibers (80–200-nm outer diameter; 30–50-nm inner diameter; 5-20-μm length; 4% metal catalyst by manufacturer)	Human bronchial epithelial cell line (BEAS 2B)	Alkaline comet assay	3.8, 19, 38, 76, 114, 228, 304, and 380 μg/mL	24, 48, 72	Significant effects observed at all concentrations for 24 h but only at some concentrations after 48 and 72 h Dose-dependent effects observed only after exposure for 48 h
Moriera et al. [85]	Cellulose nanofibers (50–1,500-nm length and 3–5-nm width)	Chinese hamster ovary cells	Alkaline comet assay	100, 500, or 1,000 μg/mL	48	No effects observed under these concentrations
Carbon nanotubes						
Folkmann et al. [61]	EliCarb SWNTs (0.9–1.7-nm diameter; length < 1 μm by manufacturer)	Female Fisher 344 rats (colon mucosa cells, liver, and lung tissues tested) by oral gavage	8-OH-dG using LC/UV/EC	0.064 or 0.64 mg/kg (dispersed in corn oil or saline)	24	Significant increases at both doses in liver and lungs but not in the colon mucosa cells
Jacobsen et al. [20]	EliCarb SWNTs (0.9–1.7 nm diameter; length < 1 μm by manufacturer)	FE1-MutaTMMouse lung epithelial cell line	Alkaline comet assay +/- FPG	100 μg/mL	3	No significant increase in the number of strand breaks but a significant increase in the number of FPG sites
Jacobsen et al. [48]	EliCarb SWNTs (0.9–1.7-nm diameter; length < 1 μm by manufacturer)	ApoE-/- mice (bronchoalveolar lavage fluid cells tested) by intratrachael instillation	Alkaline comet assay	54 μg	3	Significant increase observed
Karlsson et al. [22]	Sigma-Aldrich MWNTs (110–170 nm×5–9 μm by manufacturer)	Human lung epithelial cell line (A549)	Alkaline comet assay +/- FPG	2, 40, and 80 μg/mL (40 and 80 μg/mL for FPG)	4	Significant increase in DNA damage at 2, 40, and 80 μg/mL No significant increase in oxidatively modified lesions at 40 or 80 μg/mL No effect seen from soluble fraction from nanotubes
Kisin et al. [51]	HipCO SWNTs (99.7% carbon by mass)	Chinese hamster lung fibroblast (V79) cells	Alkaline comet assay	120, 240, and 480 μg/mL	3, 24	Significant increases only at 480 μg/mL after 3 h and 240 and 480 μg/mL after 24 h
Lindberg et al. [52]	Sigma-Aldrich carbon nanotubes (50% SWNT, 40% other nanotubes, 1.1 nm×0.5–100 μm by manufacturer)	Human bronchial epithelial cell line (BEAS 2B)	Alkaline comet assay	3.8, 19, 38, 76, 114, 228, 304, and 380 μg/mL	24, 48, 72	Significant effects observed at 3.8, 228, 304, and 380 μg/mL after 24 h and at all concentrations after 48 and 72 h

Table 1 (continued)

Reference	Nanoparticle tested (size)	Cell/organism tested	DNA damage assay	Concentrations	Exposure duration (h)	Findings
						Dose-dependent effects observed after 24 h
Pacurari et al. [54]	Carbolex SWNTs (0.8–2.0-nm diameter, 2–5-μm length by manufacturer)	Normal and malignant human mesothelial cells	H2AX, alkaline comet assay	190 and 380 μg/mL	24	Significant increases in DNA damage at both concentrations for both cell types
						No significant increase in H2AX was observed at either concentration
Pacurari et al. [53]	Bussan Nanotech Research MWNTs (81-nm diameter and 8.19-μm length)	Normal and malignant human mesothelial cells	H2AX, alkaline comet assay	12.5, 25, and 50 μg/mL (H2AX), 190 and 380 μg/mL (comet assay)	24	Significant increases in DNA damage observed at 190 and 380 μg/mL for both cells with dose–response behavior observed
						Significant increases in H2AX phosphorylation at 12.5 and 25 μg/mL but not 50 μg/mL for both cells
Yang et al. [46]	COCC SWNTs (8-nm diameter; < 5-μm length; 99.99% carbon purity)	Primary mouse embryo fibroblasts	Alkaline comet assay	5 and 10 μg/mL	24	Significant effects at both concentrations
Zeni et al. [55]	HeJi SWNTs (1.1-nm outer diameter, 50-μm length by manufacturer)	Human peripheral blood lymphocytes	Alkaline comet assay	1, 5, and 10 μg/mL	6	No effects observed
Zhu et al. [56]	Tsinghua and Nanfeng Chemical Group Cooperation MWNTs	Mouse embryo stem cells	H2AX	100 μg/mL	24	Double-strand damage observed
Fullerenes						
Dhawan et al. [75]	C_{60} dispersed in water	Human lymphocytes	Alkaline comet assay	0.022, 0.22, 2.2, 11, 22, 55, and 110 μg/L	3, 6	Significant effects consistently observed at concentrations of 2.2 μg/L and higher after 3 and 6 h
	C_{60} after solvent exchange with ethanol			0.42, 4.2, 42, 210, 420, 1,050, and 2,100 μg/L	3, 6	Significant effects observed at concentrations of 42 μg/L and higher after 3 and 6 h
Folkmann et al. [61]	C_{60} 99.9% pure by manufacturer	Female Fisher 344 rats (colon mucosa cells, liver, and lung tissues tested) by oral gavage	8-OH-dG using LC/UV/EC	0.064 or 0.64 mg/kg (dispersed in corn oil or saline)	24	Significant increases at both concentrations in the liver, at 0.64 mg/kg in lung, but no changes in the colon mucosa cells
Jacobsen et al. [20]	Sigma-Aldrich C_{60} (99.9% pure by manufacturer)	FE1-MutaTMMouse lung epithelial cell line	Alkaline comet assay +/- FPG	100 μg/mL	3	No significant increase in the number of strand breaks but a significant increase in the number of FPG sites

Jacobsen et al. [48]	Sigma-Aldrich C_{60} (99.9% pure by manufacturer)	ApoE-/- mice (bronchoalveolar lavage fluid cells tested) by intratrachael instillation	Alkaline comet assay	54 μg	3	No significant increase
Totsuka et al. [49]	Sigma-Aldrich C_{60} (99.9% pure by manufacturer)	Male C57Bl/6 J mice (lungs tested) by intratrachael instillation	Alkaline comet assay	0.05 and 0.2 mg per animal	3, 24	For 3 h, there was a significant increase for 0.2 mg but not 0.05 mg Decrease from 3 to 24 h suggesting that repair enzymes may be working
Metal nanoparticles						
Cobalt nanoparticles						
Colognato et al. [86]	Co (100–500 nm)	Human peripheral blood leukocytes	Alkaline comet assay	0.59, 2.9, and 5.9 μg/mL	2	No effects observed for Co^{2+} but significant effects observed at 2.9 and 5.9 μg/mL for Co nanoparticles
Ponti et al. [87]	Co (20–500 nm with peak at 80 nm)	Mouse fibroblast cells (Balb/3 T3)	Alkaline comet assay	0.059, 0.18, and 0.29 μg/mL	2	Statistically significant increase at all concentrations for Co nanoparticles and ions Co nanoparticles did not have a dose-dependent effect but Co ions did
Zhang et al. [108]	Inabata Co (10–30 nm, composed of Co and Co_3O_4)	Plasmid DNA	Plasmid DNA nicking	56, 560, and 1,100 μg/mL	8	Substantial DNA damage which was decreased with hydroxyl scavenger mannitol
Cobalt/chromium nanoparticles						
Bhabra et al. [91]	CoCr (nanoparticles 29.5±6.3 nm; microparticles 2.9±1.1 μm)	Human BJ fibroblasts and BeWo b30 cells (BeWo cells were used as a barrier for BJ fibroblasts)	Alkaline comet assay, H2AX	0.08 and 0.8 mg/mL (concentration for BeWo cells but less below barrier)	24	Significantly elevated DNA damage concentrations observed for fibroblasts for ions and nanoparticles at both concentrations and microparticles at 0.8 mg/mL only There was also an increase in the number of double-strand lesions for fibroblasts as measured by H2AX at both concentrations for nanoparticles and microparticles Co and Cr ions caused these effects too for the comet assay but only Cr ions had this effect for the H2AX assay
Papageorgiou et al. [90]	CoCr (nanoparticles 29.5±6.3 nm; microparticles 2.9±1.1 μm)	Primary human dermal fibroblasts	Alkaline comet assay, 8-OH-dG by immunohistochemistry	3.85×10^{-6} mg/mL to 77.0 mg/mL by orders of magnitude	24, 72, 120	Nanoparticles caused significantly more DNA damage than microparticles at higher doses after 24 h, but microparticles caused more damage after 72 h

Table 1 (continued)

Reference	Nanoparticle tested (size)	Cell/organism tested	DNA damage assay	Concentrations	Exposure duration (h)	Findings
						Dose-dependent DNA damage after 24 h for nanoparticles and microparticles
Papageorgiou et al. [90]						Dose-dependent trend was less clear for 3 and 5 days
						Microparticles indicated increased 8-OH-dG levels at concentrations of 3.85 and 38.5 mg/mL after both 3 and 24 h, and the concentrations were generally larger than those for the nanoparticles
						Nanoparticles only seemed to increase 8-OH-dG levels at 3.85 and 38.5 mg/mL after 24 h
Copper nanoparticles						
Midander et al. [94]	< 100 nm and Outokumpu Copper (<20 μm by manufacturer)	Human lung epithelial cell line (A549)	Alkaline comet assay	80 μg/mL	4	Significantly increased DNA damage from Cu nanoparticles but not Cu microparticles, but some of this damage may be from the high cytotoxicity of the Cu nanoparticles
						No effects observed from dissolved copper fraction from the particles
Gold nanoparticles						
Grigg et al. [103]	8±2 nm	Human monocyte cell line (Mono Mac 6) exposed at air-tissue interface	Alkaline comet assay	5.4 μg/cm^2	24	Significant increase observed
Jacobsen et al. [48]	2 nm	ApoE-/- mice (bronchoalveolar lavage fluid cells tested) by intratrachael instillation	Alkaline comet assay	0.54 μg	3	No significant increase
Kang et al. [104]	4, 15, 100, and 200 nm	Mouse lymphoblasts (L5178Y)	Alkaline comet assay	25, 50, and 100 μg/mL	2	Significant effects for 100- and 200-nm nanoparticles at all concentrations but not for 4- and 15-nm nanoparticles
Li et al. [105]	20 nm	Fetal lung fibroblasts (MRC-5)	8-OH-dG using LC/UV/EC	0.5 and 1 nM (25–50, 50–100 μg/mL)	72	Increase in lesions at 1 nM but not 0.5 nM

Iron nanoparticles						
Grigg et al. [103]	2 nm	Human monocyte cell line (Mono Mac 6) and rat alveolar macrophages exposed at air-tissue interface	Alkaline comet assay	0.51, 2.04, 5.1, and 10.2 μg/cm^2	24	Dose-dependent increase in toxicity with significant increase only for 5.1 and 10.2 μg/cm^2 for Mono Mac 6 cells Significant increase for rat alveolar macrophages at 10.2 μg/cm^2
Nickel nanoparticles						
Zhang et al. [108]	Inabata Co (10–30 nm)	plasmid DNA	Plasmid DNA nicking	56, 560, and 1,100 μg/mL	8	Substantial DNA damage was observed
Platinum nanoparticles						
Pelka et al. [109]	Pt particles (< 20, < 100, and >100 nm)	Human colon carcinoma cell line (HT29)	Alkaline comet assay +/- FPG	0.00048, 0.0048, 0.048, 0.48, 4.8, 48, 480, and 4,800 ng/mL	3, 24	Significant increases only observed after 3 h for 20-nm particles at 0.86 and 8.6 ng/mL and for < 100-nm particles at 8.6 ng/mL with and without FPG After 24 h, significant increases only observed for 20-nm particles and > 100-nm particles at 8.6 ng/mL with and without FPG No significant effects observed for >100-nm particles
Silver nanoparticles						
Ahamed et al. [113]	25 nm with and without polysaccharide coating	Mouse embryonic stem and mouse embryonic fibroblast cells	H2AX	50 μg/mL	24, 48, 72	Increase in phosphorylation for both cells at all time points Intensity appeared to be greater for coated nanoparticles
AshaRani et al. [114]	Starch-capped Ag nanoparticles (6–20 nm)	Human glioblastoma cells (U251) and normal human fibroblasts (IMR-90)	Alkaline comet assay	25, 50, 100, 200, and 400 μg/mL	48	Concentration-dependent effects for U251 cells which were significant after 50 μg/mL Concentration-dependent effects for IMR-90 cells up to 100 μg/mL and then no further increase Significant effects at all concentrations for the IMR-90 cells
Grigg et al. [103]	5.5±1.5 nm	Human monocyte cell line (Mono Mac 6) exposed at air-tissue interface	Alkaline comet assay	3.4 μg/cm^2	24	Significant increase observed
Kim et al. [115]	Nanopoly (< 10-nm diameter by manufacturer)	Human hepatoma cells (HepG2)	H2AX	1 and 2 μg/mL	24	Dose dependence observed and increased damage

Table 1 (continued)

Reference	Nanoparticle tested (size)	Cell/organism tested	DNA damage assay	Concentrations	Exposure duration (h)	Findings
						10 mM antioxidant *N*-acetylcysteine stopped damage from nanoparticles and decreased damage to cells treated with $AgNO_3$
Sawosz et al. [116]	Nano-Tech (2–6 nm)	Chicken eggs (embryos)	8-OH-dG using LC/UV/EC	15 μg/egg	20 days	No increase in liver concentration of 8-OH-dG
Silver–copper nanoparticles						
Sawosz et al. [116]	Nano-Tech (2–6 nm)	Chicken eggs (embryos)	8-OH-dG using LC/UV/EC	15 μg/egg	20 days	No increase in liver concentration of 8-OH-dG
Silver–palladium nanoparticles						
Sawosz et al. [116]	Nano-Tech (2–6 nm)	Chicken eggs (embryos)	8-OH-dG using LC/UV/EC	15 μg/egg	20 days	No increase in liver concentration of 8-OH-dG
Metalloid nanoparticles						
Germanium nanoparticles						
Lin et al. [73]	Ge nanoparticles (approximately 1–10, 20–50, and 100–200 nm in diameter)	Chinese hamster ovary (CHO) K1 cells	Alkaline comet assay, H2AX	0.36 mg/mL	0, 12	There was apparent damage by comet assay after 0 h for the Ge nanoparticles but not for GeO_2, and significant damage for Ge nanoparticles after 12 h
						No difference was observed for γ-H2AX formation after Ge nanoparticle or GeO_2 addition, which suggests a potential artifact for the comet assay
						Effects of radiation after Ge nanoparticle addition were also observed, and Ge nanoparticles had a radiosensitizing effect similar to that of GeO_2
Silica nanoparticles						
Barnes et al. [122]	Si nanoparticles (nominal sizes 30, 80, and 400 nm), two batches of colloidal nanoparticles from SigmaLudox (20-40 nm)	Mouse embryo fibroblast cell line (3 T3-L1)	Alkaline comet assay	4 and 40 μg/mL	3, 6, 24	No significant effects observed after any time period for any silicon dioxide particle
						Independently validated at two separate laboratories
Gerloff et al. [44]	Sigma SiO_2 (14-nm primary particle size by manufacturer)	Human carcinoma intestinal cells (Caco-2 cells)	Alkaline comet assay +/- FPG	133.3 μg/mL	4	Significant increase observed with FPG but not without FPG

Jin et al. [123]	Si nanoparticles (50±3 nm)	Human lung epithelial cell line (A549)	Alkaline comet assay, pulse field gel electrophoresis, agarose gel electrophoresis using genomic DNA strands, 8-OH-dG using western blot	0.1, 1, 10, 100, 500 μg/mL	48, 72	No effects observed at any concentration
Lee et al. [125]	Sigma-Aldrich (7 and 10 nm by manufacturer)	*Daphnia magna* and *Chironomus riparius*	Alkaline comet assay	1 μg/mL	24	No significant increase
Wang et al. [124]	Sigma-Aldrich SiO_2 (7–9 nm)	Human B-cell lymphoblastoid cell line (WIL2-NS)	Alkaline comet assay	60 and 120 μg/mL	24	Significant damage was not observed
Yang et al. [46]	Runhe (20.2±6.4 nm; >99.0% purity)	Primary mouse embryo fibroblasts	Alkaline comet assay	5 and 10 μg/mL	24	Significant effects at both concentrations
Metal oxide nanoparticles						
Aluminum oxide nanoparticles						
Balasubramanyam et al. [127]	Sigma-Aldrich Al_2O_3 (30 and 40 nm)	Female Wistar rats (whole blood from retro-orbitus was tested) by gavage	Alkaline comet assay	500, 1,000, and 2,000 mg/kg by gavage	4, 24, 48, 72	Significant effects observed at 1,000 and 2,000 mg/kg, but not 500 mg/kg, after 4 and 24 h for 30- and 40-nm particles No significant effects observed for bulk particles at any time or concentration No significant effects observed for any particle size or concentration after 72 h
Kim et al. [126]	Sigma-Aldrich Al_2O_3 (< 50 nm)	Mouse lymphoma cell line (L5178Y) and human bronchial epithelial cells (BEAS-2B)	Alkaline comet assay	1,250, 2,500, and 5,000 μg/mL for L5178Y cells 68.36, 136.72, and 273.44 μg/mL for BEAS-2B cells with S-9 and 97.66, 195.32, and 390.63 μg/mL without S-9	2	Significant damage to L5178Y cells with S-9 at all concentrations and only at 2,500 μg/mL without S-9 Significant damage to BEAS-2B cells at all concentrations with and without S-9
Cerium oxide nanoparticles						
Auffan et al. [130]	Nano-CeO_2 (Rhodia Chemicals; 7 nm) and micro-CeO_2 (320 nm)	Normal human fibroblasts	Alkaline comet assay	0.006, 0.06, 0.6, 6, 60, 600, and 1,200 μg/mL		Toxicity consistently observed for concentrations above 60 μg/mL Nano-CeO_2 was more toxic on a mass basis but equivalent on a surface area basis

Table 1 (continued)

Reference	Nanoparticle tested (size)	Cell/organism tested	DNA damage assay	Concentrations	Exposure duration (h)	Findings
						Adding antioxidant L-ergothioneine decreased DNA damage and significant results only occurred at 1,200 μg/mL
Lee et al. [125]	15 and 30 nm	*Daphnia magna* and *Chironomus riparius*	Alkaline comet assay	1 μg/mL	24	Significant increase for 15 nm only for *Chironomus riparius* and for both sizes for *Daphnia magna*
Pierscionek et al. [128]	10–12 nm	Human lens epithelial cell line (CRL-11421)	Alkaline comet assay	5 and 10 μg/mL	24	No significant effects observed
Rothen-Rutishauser et al. [129]	CeO_2 (mean primary particle diameter 5–20 nm)	Human lung epithelial cell line (A549)	8-OH-dG using oxyDNA assay kit	NA (cells exposed in glovebox exposure setup)	10, 20, and 30 minutes	Significant increase in percent of cells with 8-OH-dG after 20 and 30 min
Copper oxide nanoparticles						
Karlsson et al. [22]	Sigma-Aldrich CuO (42 nm by manufacturer)	Human lung epithelial cell line (A549)	Alkaline comet assay +/- FPG	2, 40, and 80 μg/mL (40 and 80 μg/mL for FPG)	4	Significant increases in DNA damage at 40 and 80 μg/mL but not 2 μg/mL Highest among all nanoparticles tested in this study Significant increase in oxidative lesions only at 80 μg/mL Dose-dependent DNA damage and oxidatively modified lesion patterns observed
Karlsson et al. [23]	Sigma-Aldrich CuO (20–40 nm and 0.5–10 μm)	Human lung epithelial cell line (A549)	Alkaline comet assay +/- FPG	40, 80 μg/mL	4	Nanoparticles caused significantly more DNA damage than microparticles at 80 μg/mL and almost at 40 μg/mL (p=0.051) Significantly increased DNA damage for nanoparticles and microparticles at both concentrations Nanoparticless caused significantly more FPG lesions only at 80 μg/mL compared with the control No significant increase in the number of FPG lesions compared with controls for microparticles at either concentration
Midander et al. [94]	Sigma-Aldrich (28 nm and 2.9 μm)	Human lung epithelial cell line (A549)	Alkaline comet assay	80 μg/mL	4	Increase in DNA damage from CuO nanoparticles and

						microparticles, but significantly more damaged from the nanoparticles than the microparticles
						No effects observed from copper fraction dissolved from the particles
Iron oxide nanoparticles						
Auffan et al. [133]	Fe_2O_3 (maghemite) (6 nm)	Normal human fibroblasts	Alkaline comet assay	0.001, 0.01, 0.1, 1, 10, and 100 μg/mL	2, 24	No significant effects observed
Bhattacharya et al. [134]	Hematite (Fe_2O_3; ~50-nm hydrodynamic radius)	Human diploid fibroblasts (IMR-90), human bronchial epithelial cells (BEAS-2B)	Alkaline comet assay, 8-OH-dG using ELISA	10, 25, 50, and 250 μg/mL (comet assay), 25 and 50 μg/mL (8-OH-dG)	24	Significantly increased DNA damage by comet assay at 50 and 250 μg/mL for IMR-90 cells and 250 μg/mL for BEAS-B2 cells
						No significant increase in 8-OH-dG was observed
Karlsson et al. [22]	Sigma-Aldrich Fe_2O_3 (29 nm by manufacturer)	Human lung epithelial cell line (A549)	Alkaline comet assay +/- FPG	2, 40, and 80 μg/mL (40 and 80 μg/mL for FPG)	4	No significant increase in DNA damage
Karlsson et al. [22]	Sigma-Aldrich Fe_3O_4 (20–30 nm by manufacturer)	Human lung epithelial cell line (A549)	Alkaline comet assay +/- FPG	2, 40, and 80 μg/mL (40 and 80 μg/mL for FPG)	4	No significant increase in SSBs
						Significant increase in the number of oxidatively modified lesions at 80 μg/mL
Karlsson et al. [23]	Sigma-Aldrich Fe_2O_3 (30–60 nm and 0.15–1 μm)	Human lung epithelial cell line (A549)	Alkaline comet assay +/- FPG	40 and 80 μg/mL	4	Significant DNA damage from microparticles but not nanoparticles at 80 μg/mL, and there was a significant difference between the two particle types
						No significant increase in DNA damage for either particle at 40 μg/mL
						No significant increase in the number of oxidatively modified lesions for either particle type at either concentration
Karlsson et al. [23]	Sigma-Aldrich Fe_3O_4 (20–40 nm and 0.1–0.5 μm)	Human lung epithelial cell line (A549)	Alkaline comet assay +/- FPG	40, 80 μg/mL	4	Significant increase in DNA damage from microparticles at 40 and 80 μg/mL but not from nanoparticles
						Nanoparticles caused significantly more oxidatively modified lesions than microparticles at

Table 1 (continued)

Reference	Nanoparticle tested (size)	Cell/organism tested	DNA damage assay	Concentrations	Exposure duration (h)	Findings
						80 μg/mL, and the number was significant compared with controls only at 80 μg/mL
Magnesium oxide nanoparticles						
Gerloff et al. [44]	Nanoscale Materials MgO (8-nm primary particle size by manufacturer)	Human carcinoma intestinal cells (Caco-2 cells)	Alkaline comet assay +/- FPG	133.3 μg/mL	4	No effect observed
Titanium dioxide nanoparticles						
Bhattacharya et al. [134]	Degussa anatase (91-nm hydrodynamic radius)	Human diploid fibroblasts (IMR-90), human bronchial epithelial cells (BEAS-2B)	Alkaline comet assay, 8-OH-dG using ELISA	10, 25, 50, and 250 μg/mL (comet assay), 25 and 50 μg/mL (8-OH-dG)	24	Increased 8-OH-dG formation at 25 and 50 μg/mL for IMR-90 cells
						No effect on DNA damage by comet assay with either cell line
Falck et al. [148]	Nanosized rutile (10 um×40 nm), nanosized anatase (< 25 nm), and bulk rutile (< 5 um) all from Sigma, all sizes from manufacturer	Human bronchial epithelial cells (BEAS-2B)	Alkaline comet assay	3.8, 19, 38, 76, 114, 228, 304, and 380 μg/mL	24, 48, 72	Nanosized anatase and bulk rutile were similarly effective, whereas nanosized rutile was less effective, but none of them were a potent inducer of DNA damage
						Elevated DNA damage was observed at various concentrations but trends were not clear
						Dose-dependent patterns were observed after some exposure periods but not others and a clear trend was not observed
Gerloff et al. [44]	Degussa P25 (20–80 nm), Aldrich Fine (40–300 nm; pure anatase), and TiO_2-HAS (< 10 nm)	Human carcinoma intestinal cells (Caco-2 cells)	Alkaline comet assay +/- FPG	133.3 μg/mL	4	TiO_2 slides were processed in total darkness or normal laboratory lighting, and laboratory lighting caused a significant increase in DNA damage and the number of FPG-sensitive lesions
						No effect in dark for TiO_2 of any size and no difference among different sizes
Gopalan et al. [146]	Sigma-Aldrich TiO_2 (anatase; 40–70 nm)	Human sperm and lymphocyte cells	Alkaline comet assay	3.73, 14.92, 29.85, 59.7 μg/mL	0.5	Significant increases in DNA damage at all concentrations

		(cells were spiked in the dark, preirradiated with UV light, or exposed to UV light after nanoparticle addition)				for both cells under each condition For sperm cells, no differences observed as a result of UV exposure except for preirradiation followed by addition of 3.73 μg/mL TiO_2 nanoparticles For lymphocytes, there was a statistically significant increase from UV exposure at the highest three doses compared with dark conditions
Gurr et al. [19]	Sigma-Aldrich anatase at 10, 20, 200, and ≥200 nm and Kanto Chemical rutile at 200 nm, manufacturer sizes	Human bronchial epithelial cells (BEAS-2B) exposed in total darkness	Alkaline comet assay +/- FPG	5 and 10 μg/mL preliminary experiment 10 μg/mL primary experiment	1	In an experiment with 10-nm anatase and >200-nm anatase, increased damage was observed only at 10 μg/mL for 10-nm particles Significant increase in damage for 10- and 20-nm anatase and 200-nm rutile but not for 200-nm anatase or >200-nm anatase A mixture of 1:1 200-nm anatase and rutile caused more damage than an equivalent total mass of either of them by themselves
Kang et al. [149]	Degussa P25 (25 nm by manufacturer)	Peripheral blood lymphocytes	Alkaline comet assay	20, 50, or 100 μg/mL	6, 12, 24	TiO_2 caused significant DNA damage at each concentration and each time point The addition of 1 mM *N*-acetylcysteine significantly decreased DNA damage
Karlsson et al. [22]	Sigma-Aldrich TiO_2 (63 nm by manufacturer)	Human lung epithelial cell line (A549)	Alkaline comet assay +/- FPG	2, 40, and 80 μg/mL (40 and 80 μg/mL for FPG)	4	Significant increase in DNA damage only at 80 μg/mL No significant increase in the number of oxidatively modified lesions
Karlsson et al. [23]	Sigma-Aldrich TiO_2 (20–100 nm and 0.3–1 μm)	Human lung epithelial cell line (A549)	Alkaline comet assay +/- FPG	40, 80 μg/mL	4	Significantly more DNA damage from microparticles than nanoparticles at 80 μg/mL Significant DNA damage increases at 40 and 80 μg/mL for microparticles and 80 μg/mL for nanoparticles

Table 1 (continued)

Reference	Nanoparticle tested (size)	Cell/organism tested	DNA damage assay	Concentrations	Exposure duration (h)	Findings
						No significant increase in the number of oxidatively modified lesions for either particle type at either concentration
Lee et al. [125]	Sigma-Aldrich (7 and 20 nm by manufacturer)	*Daphnia magna* and *Chironomus riparius*	Alkaline comet assay	1 μg/mL	24	No significant increase
Nakagawa et al. [141]	Nippon Aerosil p-25 (anatase, 21 nm), Wako WA (anatase, 255 nm), Wako WR (rutile, 255 nm), TP-3 (rutile, 420 nm), sizes by manufacturer	Mouse lymphoma cells (L5178Y)	Alkaline comet assay	3.1, 12.5, 50, 200, 800, and 3,200 μg/mL	1 h dark and 50 min with or without UV	Only WA caused DNA damage without UV irradiation
						p-25 was the most potent with irradiation while WR was the least
						Increasing UVA irradiation energies lead to increased DNA damage for a fixed p-25 concentration
Reeves et al. [142]	Sigma (5 nm, anatase)	Goldfish (*Carassius auratus*) skin cells (GFSk-S1)	Alkaline comet assay +/- FPG and endonuclease III	1, 10, and 100 μg/mL	2, 24	No significant increase for endonuclease III lesions after 24 h without UVA at any concentration
						Significant increase for FPG lesions at all concentrations after 24 h without UVA
						Significant increase only at 100 μg/mL without FPG or endonuclease III after 24 h without UVA
						After 2 h, significant increases were observed with and without FPG for UVA only, for 10 μg/mL TiO_2 only, and further significantly increased for TiO_2 with UVA
Rehn et al. [153]	Degussa (P25 and T805)	Female Wistar rats (lungs tested) by intratracheal installation	8-OH-dG using immunocytological assay	0.15, 0.3, 0.6, and 1.2 mg/lung	90 days	No significant effects observed at any concentration for P25 or T805
Serpone et al. [143]	Many types of TiO_2 (some modified to passivate the surface to	Plasmid DNA and human keratinocytes	Plasmid DNA nicking, alkaline comet assay	50, 100, 500, 1,000, 5,000, 10,000, and 20,000 μg/mL	10, 20, 30, 40, or 60 min	Modified TiO_2 did not cause an increase in DNA damage after irradiation for the

	minimize or suppress photoactivity)					plasmid nicking assay or the comet assay compared with controls Unmodified samples generally caused an increase in plasmid DNA damage and damage by comet assay after UV irradiation Treatment of keratinocytes with TiO_2 in the dark did not cause increased DNA damage Increasing the concentration of unmodified TiO_2 increased damage for nicking assay but not in a monotonic fashion
Trouiller et al. [154]	Degussa P25 (primary particle size 21 nm)	C57B1/6Jpun/pun mice	Alkaline comet assay, 8-OH-dG using LC/UV/EC, H2AX	500 mg/kg (comet assay and 8-OH-dG), 50, 100, 250, and 500 mg/kg (H2AX)	5 days	Significant increases in DNA damage by comet assay and 8-OH-dG measurements at 500 mg/kg Significant increases for a number of phosphorylated cells by γ-H2AX in a dose-dependent manner
Vevers et al. [144]	Degussa P25 (24.4±0.5 nm)	Rainbow trout (*Oncorhyncus mykiss*) gonad cells (RTG-2)	Alkaline comet assay +/- FPG	5 or 50 μg/mL	4	TiO_2 caused a significant reduction in DNA damage when UVA was not used Significantly increased DNA damage was observed in minimal essential medium with TiO_2 and UVA When FPG was included, only 50 μg/mL with UVA significantly increased oxidative lesions
Wang et al. [150]	Sigma-Aldrich TiO_2 (6–10 nm, 99% purity)	Human B-cell lymphoblastoid cell line (WIL2-NS)	Alkaline comet assay	65 μg/mL	24	Significant increase in DNA damage observed
Zhang et al. [108]	Inabata TiO_2 (10–30 nm)	Plasmid DNA	Plasmid DNA nicking	56, 560, and 1,100 μg/mL	8	Minimal damage observed
Zhu et al. [145]	10–20 nm and 50–60 nm anatase, 50–60 nm rutile	Teasy plasmid DNA exposed to UV radiation	Plasmid DNA nicking and 8-OH-dG by LC/UV/EC	100 μg/mL	0.25	No damage was observed after only UV irradiation for 8-OH-dG or gel electrophoresis Significant increases in DNA damage by both measures were observed for each type of nanoparticle

Table 1 (continued)

Reference	Nanoparticle tested (size)	Cell/organism tested	DNA damage assay	Concentrations	Exposure duration (h)	Findings
						For both measurements, 10–20-nm anatase>50–60-nm anatase > 50–60-nm rutile
Zinc oxide nanoparticles						
Gerloff et al. [44]	Nanoscale Materials (10 nm) or Nanostructured and Amorphous Materials (20 nm), both sizes by manufacturer	Human carcinoma intestinal cells (Caco-2 cells)	Alkaline comet assay +/- FPG	133.3 μg/mL	4	Significant effects observed with and without FPG
						Different sizes of ZnO particles all caused DNA damage except for the largest particles without FPG at a concentration of 133.3 μg/mL
						No significant differences were observed in the DNA damage potential of the various particles
Gopalan et al. [146]	Sigma-Aldrich ZnO (40-70 nm)	Human sperm and lymphocyte cells (cells were spiked in the dark, preirradiated with UV light, or exposed to UV light after nanoparticle addition)	Alkaline comet assay	11.5, 46.2, 69.4, and 92.3 μg/mL	0.5	Statistically significant results were observed at all concentrations for both cells except for the lowest concentration in the dark for sperm cells
						For sperm cells, there was only a statistically significant difference at 11.5 μg/mL for samples treated with UV light compared with those in the dark
Karlsson et al. [22]	Sigma-Aldrich ZnO (71 nm by manufacturer)	Human lung epithelial cell line (A549)	Alkaline comet assay +/- FPG	2, 40, and 80 μg/mL (40 and 80 μg/mL for FPG)	4	Significant increase in DNA damage and number of oxidatively modified lesions at only 80 μg/mL
Lin et al. [155]	Sigma (70±13- and 420±269-nm ZnO)	Human lung epithelial cell line (A549)	Alkaline comet assay	10, 12, and 14 μg/mL	24	No significant difference between particle sizes but hydrodynamic radii were similar for the two particles in this concentration range
						Significant effects observed at all concentrations for both types of particles
						Steep dose response observed

Sharma et al. [156]	Sigma-Aldrich (30 nm by TEM)	human epidermal cell line (A431)	Alkaline comet assay	0.001, 0.008, 0.08, 0.8, and 5 μg/ml	6	Significant increase observed only for 0.8 and 5 μg/mL
Yang et al. [46]	Nanuo 19.6±5.8 nm (>99.9% purity)	Primary mouse embryo fibroblasts	Alkaline comet assay	5 and 10 μg/mL	24	Significant effects at both concentrations
Additional metal oxide nanoparticles						
Karlsson et al. [22]	Sigma-Aldrich $CuZnFe_2O_4$ (29 nm by manufacturer)	Human lung epithelial cell line (A549)	Alkaline comet assay +/- FPG	2, 40, 80 μg/mL (40, 80 μg/mL for FPG)	4	Significant increases in DNA damage and number of oxidatively modified lesions only at 40 and 80 μg/mL
Quantum dots						
Anas et al. [160]	Invitrogen streptavidin-functionalized CdSe–ZnS quantum dots	Plasmid DNA	Plasmid DNA nicking +/- FPG and +/- endonuclease III	0.5 nM	1	DNA damage was not observed in the dark with quantum dots but was observed after photosensitizing the quantum dots Similarly, the photosensitized quantum dots were also shown to damage purine and pyrimidine bases, whereas no effects were observed in the dark
Jacobsen et al. [48]	American Dye Source positively and negatively charged quantum dots (4.5–5.5 nm by manufacturer)	ApoE-/- mice (bronchoalveolar lavage fluid cells tested) by intratrachael instillation	Alkaline comet assay	63 μg Cd	3	Significant increases observed and approximately the same values for positive and negative surface charges
Gagné et al. [162]	CdTe quantum dots (American Dye Source)	*Elliptio complanata* mussels tested gills and digestive glands	Alkaline comet assay+alkaline precipitation assay	1.6, 4 and 8 μg/mL	24	Significant increase in gills at 1.6 and 4 μg/mL but not 8 μg/mL Significant increase in digestive gland at 4 and 8 μg/mL Significant DNA damage for 0.5 μg/mL Cd for digestive glands but not gills
Gagné et al. [163]	CdTe with cysteamine coating, aged for 2 months or 2 years before exposure	Rainbow trout (*Oncorhynchus mykiss*) hepatocytes	Alkaline comet assay+alkaline precipitation assay	0.4, 2, 10, 50, and 250 μg/mL	48	For quantum dots aged for 2 months, significant increases in DNA damage for 0.4, 10, and 50 μg/mL but not for 2 or 250 μg/mL
Gagné et al. [163]						For quantum dots aged for 2 years, DNA damage was only significantly increased at 2 μg/mL For quantum dots aged for 2 months only, there was a correlation between DNA damage results and labile zinc/cadmium concentrations
Green and Howman [158]	Cambridge Bioscience CdSe quantum dots (605 biotin conjugate)	Supercoiled double strands of DNA	Plasmid DNA nicking	2 μM	0.25, 0.5, 0.75, and 1	DNA nicking occurred with and without UV light, but more occurred with UV light

Table 1 (continued)

Reference	Nanoparticle tested (size)	Cell/organism tested	DNA damage assay	Concentrations	Exposure duration (h)	Findings
Hoshino et al. [159]	ZnS-coated CdSe quantum dots coated with 11-mercaptoundecanoic acid (QD-COOH), cysteamine (QD-NH_2), or thioglycerol (QD-OH) or QD-OH/COOH, and QD-NH2/OH	Human lymphoma cells (WTK1)	Alkaline comet assay	0.5, 1, 1.5, and 2 μM	2 and 12	Significant increase in damage observed after 2 h but not 12 h for QD-COOH only at 2 μM Purifying QD-COOH decreased DNA damage Other quantum dots at 4 μM concentrations did not cause DNA damage after 2 h Impurities in the synthesis process also caused DNA damage

Concentration units are typically given in mass of nanoparticle per volume of medium unless otherwise specified.

8-OH-dG 8-hydroxy-2′-deoxyguanosine, *LC/UV/EC* liquid chromatography with UV and electrochemical detection, *FPG* formamidopyrimidine glycosylase, *SWNT* single-walled carbon nanotube, *MWNT* multi-walled carbon nanotube, *ELISA* enzyme-linked immunosorbent assay, *TEM* transmission electron microscopy

base lesions (including 8-OH-dG) in individual DNA samples. The capability and importance of monitoring the formation of 8-OH-dG is significant because of its known mutagenic and promutagenic activity, as it can cause G→T transversion mutations that are found in dysfunctional genes associated with cancer [33]. However, there exist a number of other oxidatively induced base lesions that are equally mutagenic, but often more difficult to accurately detect because of their low levels. For example, among the pyrimidine lesions, 5-hydroxycytosine and 5-hydroxyuracil are both highly mutagenic lesions, leading to C→T transition mutations [34–36]. Thymine glycol is another pyrimidine lesion that blocks DNA polymerases and is thus a lethal lesion [37]. Among the purine lesions, 2,6-diamino-4-hydroxy-5-formamidopyrimidine (FapyGua) and 4,6-diamino-5-formamidopyrimidine are potentially mutagenic, and can cause G→T and A→T mutations, respectively [38–40]. In certain cases, FapyGua may even be more mutagenic than 8-OH-dG [41]. The advantages of our mass-spectrometry-based procedures over other reported methods for evaluating oxidative damage to DNA bases are the following: (1) we can obtain absolute confirmation of the lesion's identity (type), (2) we can obtain absolute quantitative information on each individual lesion that is traceable to high-purity reference standards, and most importantly, (3) we have the capability to decipher and describe the mechanistic pathways by which specific ENs might induce oxidative damage to DNA marked by the formation of DNA base lesions. In one of our present studies, we are utilizing GC/MS procedures to investigate the effect of copper oxide (CuO) nanoparticles (NPs) on genomic DNA damage in germinating plants in vivo. Thus far, we have observed remarkable trends in terms of the types and levels of oxidatively induced base lesions that are formed owing to the presence and activity of the NPs. The trends that we currently observe seem to correlate strongly with the NP dose and with the species and/or type of plant under investigation (unpublished results).

Oxidatively induced DNA damage, whether it is detected and measured as discrete strand break lesions or as DNA base lesions, is associated with biological mechanisms involved in the onset of carcinogenesis, mutagenesis, and premature aging in humans. Thus, it is imperative to describe and understand the mechanisms by which ENs could potentially mediate and/or promote these disease processes. Hence, this paper has two specific aims: (1) to review and assess the mechanistic details of EN-induced oxidative damage to DNA as reported in the current scientific literature and (2) to review and evaluate the predominant assays and procedures that have been reported for measuring EN-induced oxidative damage to DNA. The review is specifically focused on studies that investigated ENs that were 100 nm or smaller in at least one

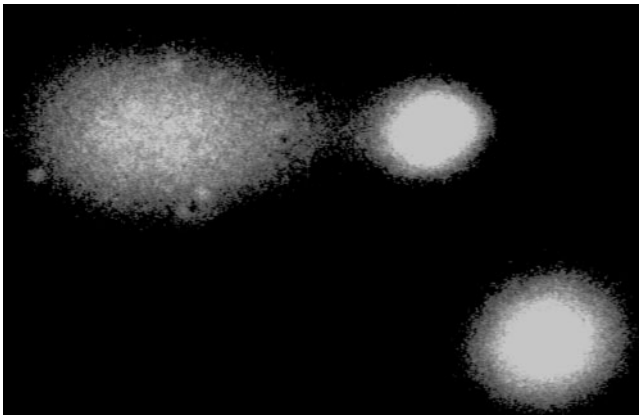

Fig. 1 Comets from the alkaline comet assay. The higher comet is representative of substantial DNA damage, whereas the lower comet indicates minimal DNA damage. (Reprinted with permission from Peggy Olive, British Columbia Cancer Agency)

dimension and that measured and reported oxidative damage in terms of strand break lesions and/or in terms of oxidative base lesions. Studies on incidental NPs such as ultrafines produced through combustion processes were not included. Additionally, one of the most frequently discussed suggestions for EN research involves proper characterization of the NPs [3, 6, 42, 43]. Although this review does not cover this topic in depth, the characterization methods utilized in each study on EN-induced oxidative damage to DNA are summarized in Table S1 in the Electronic supplementary material. It is clear that the extent of EN characterization spans a broad range, with many reports providing minimal characterization information. In our opinion, the lack of adequate characterization data is a likely cause for the discrepancies observed among the studies described herein. The discussion will focus on five major categories of ENs: carbonaceous, metals, metalloids, metal oxides, and semiconducting quantum dots (Qdots).

Mechanisms and measurements

Carbon-based nanomaterials

Carbon-based (carbonaceous) ENs exist as a variety of structures, including tubes, spheres, particles, and fibers. Tube structures include both single-walled carbon nanotubes (SWNTs) and multi-walled carbon nanotubes (MWNTs), spheres include C_{60} fullerenes, particles include nanoparticulate carbon black (nCB), and fibers include graphite nanofibers.

Carbon black nanoparticles

The toxicity of nCB has been investigated in seven in vitro experiments [18, 21, 22, 44–47] and DNA damage was typically but not always detected. A commercially available carbon powder (larger than 30 nm) was not found to increase DNA strand breaks or Fpg-sensitive lesions at concentrations up to 80 μg/mL cell medium using A549 cells [22]; unless otherwise stated, all nanomaterial concentrations for in vitro assays will have units of mass of nanomaterial per volume of cell medium. However, Printex 90 was shown to induce SSBs in A549 cells using a concentration of 100 μg/mL [18, 45]. This result appears to be due to the higher concentration tested by Mroz et al. [18, 45], but they did not test a range of concentrations to determine the concentration at which enhanced DNA damage did not occur, and thus other experimental factors in these studies could be the cause of the differing results. This same pattern of results was also observed for Fpg-sensitive sites in these studies. The lowest concentration observed to cause DNA damage by nCB was 5 μg/mL using primary mouse fibroblast cells [46], whereas concentrations as high as 786 μg/mL did not induce damage as measured by the alkaline comet assay in Chinese hamster lung fibroblasts or human embryonic lung fibroblasts [47]. It is surprising that these different results span 2 orders of magnitude and this suggests that much is yet unknown about what characteristics of nCB are most important for inducing toxicity and to what extent cell lines differ in their sensitivity to nCB exposure.

The toxicity of nCB has also been investigated in three in vivo studies using mice and rats, each of which studied

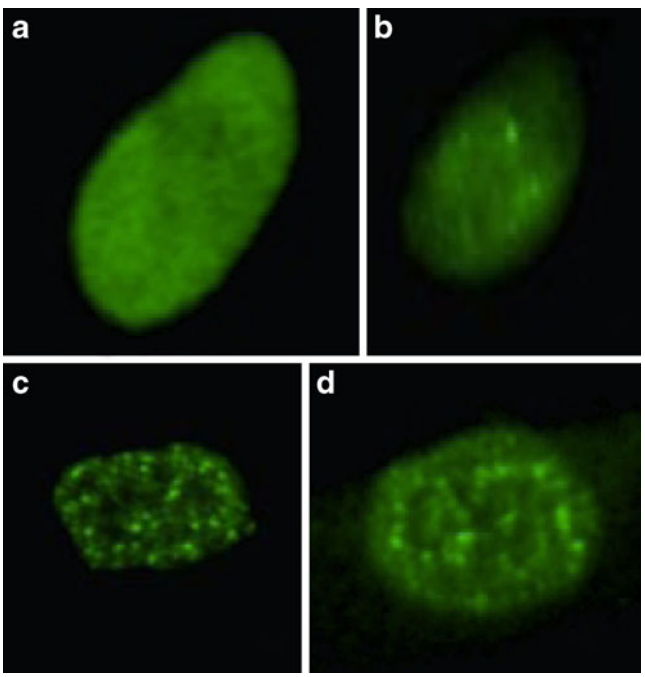

Fig. 2 WI-38 cells without any H2AX foci (*a*) and WI-38 cells with one or more foci (*b–d*). (Reprinted with permission from [173])

inhalation exposure risks. In the two studies in which the exposure was through intratracheal installation, significant increases in SSBs were detected using the alkaline comet assay [48, 49]. However, the concentration needed to induce these lesions differed between the studies. SSBs were detected by Totsuka et al. [49] after addition of 200 μg per mouse but not 50 μg per mouse, whereas exposing each mouse to 54 μg did induce DNA damage in a study by Jacobsen et al. [48]. Both of these studies utilized the alkaline comet assay to detect SSBs induced by Printex 90 NPs, and thus this different response could be a result of the types of mice tested. Gallagher et al. [50] also tested the toxicity of Printex 90 NPs with rats but used an inhalation exposure setup. Elevated concentrations of 8-OH-dG measured by LC/UV detection or LC/UV/EC detection were detected only after the highest exposure concentration of 52.8 mg/m^3 after 13 weeks of exposure, although elevated concentrations of 8-OH-dG were also detected at a concentration of 7.1 mg/m^3 after an additional 44-week recovery period in which the rats were not exposed. This result suggests that the continued presence of nCB in the lungs poses a serious long-term risk.

nCB is hypothesized to cause oxidative stress and induce oxidative damage to DNA in in vitro systems on the basis of its small size and biopersistence, metal content, and/or polycyclic aromatic hydrocarbon (PAH) content [2]. Biopersistence relates to the small size of nCB and its capacity to enter cells, and the expected slow rate at which the NP is eliminated or excreted by the organism. Biopersistence could lead to the induction of inflammation and activation of ROS-producing neutrophils and other inflammatory cells as discussed previously. nCB, owing to its large surface area, also has the potential to adsorb transition metals (i.e., Fe, Ni, Cu, Cr, etc.) onto its surface that could catalyze Fenton-like reactions to produce •OH. And finally, owing to its physical structure (large surface area), nCB has the capacity to adsorb large quantities of PAHs onto its surface. PAHs can be converted to quinones via biotransformation reactions and quinones are active redox-cyclers (quinone ↔ semiquinone) and generators of $O_2^{\bullet-}$. The $O_2^{\bullet-}$ can dismutate to H_2O_2, which can react with transition metal ions to produce •OH [7]. Remarkably, not a single study investigated or reported nCB-induced oxidative damage to DNA based on the potential mechanisms described above nor did any of the studies give detailed experimental information on any other potential DNA damage mechanism.

Carbon nanotubes

Despite a wide range of types of carbon nanotubes (i.e., MWNTs and SWNTs), nanotube dispersion procedures, in vivo exposure procedures, and in vitro assays using various cell types, carbon nanotubes consistently revealed the potential for induction of DNA damage. In vitro results using a variety of cell lines generally indicate DNA damage after exposure to SWNTs or MWNTs [20, 22, 46, 51–56]. These studies typically used cell lines related to the lungs given the serious concerns about carbon nanotubes having effects similar to asbestos [53, 57, 58]. DNA damage was detected using the alkaline comet assay both with and without Fpg and the γ-H2AX assay [20, 22, 46, 51–54, 56]. A significant increase in SSBs was determined by the alkaline comet assay for MWNTs at the very low concentration of 2 μg/mL [22]. However, toxicity of SWNTs to human peripheral blood lymphocytes was not detected using the alkaline comet assay at SWNT concentrations of 1, 5, and 10 μg/mL [55], and several of the other studies did not observe DNA damage with every assay [20, 22, 54]. There was not a clear trend to the genotoxic responses though. In a study by Jacobsen et al. [20], elevated levels of SSBs were not measured using the alkaline comet assay but the numbers of Fpg-sensitive base lesions were increased, whereas the opposite pattern was observed by Karlsson et al. [22]. The impact of various factors such as SWNTs versus MWNTs and the impact of different lengths of nanotubes have not been directly studied. However, potentially lethal (if not repaired) DSBs were detected using the γ-H2AX assay in two studies using MWNTs [53, 56], but DSBs were not detected in the one study that investigated DSBs using SWNTs [54]. On the basis of this limited information, MWNTs may be more genotoxic than SWNTs, but additional comparative research among different types of nanotubes and enhanced understandings of the characteristics of the nanotubes that cause toxicity are necessary before definitive conclusions are reached.

One potential artifact that was only tested in one of these studies was the potential for chemicals or metals leached from the nanotubes to cause a toxic response [22]. Although the soluble fraction was not shown to induce DNA damage in this study, yttrium released from SWNTs has been shown to impact the calcium ion channel of tsA201 cells [59], and SWNTs have previously been shown to leach substantial concentrations of nickel, which may cause significant toxic effects [60]. Assessing the potential for leached compounds to cause toxicity in future studies would help confirm that the toxicity observed results from exposure to the nanotubes themselves rather than from exposure to leached catalytic metals. If metals or organic chemicals leached from the nanotubes are revealed to cause toxic responses, purifying the nanotubes to remove these materials may be a straightforward and important step in mitigating their potential risks.

The two in vivo studies on this topic investigated rats or mice exposed to SWNTs through oral gavage or intra-

tracheal installation, respectively [48, 61]. After exposure by oral gavage, elevated levels of 8-OH-dG were detected using the LC/EC method on the liver and lung but not on colon mucosa cells after 24 h at doses of 0.064 and 0.64 mg/kg body mass [61]. It is unclear though why DNA damage was observed in some organs but not others. This may be a result of the biodistribution of the NPs within the organism after exposure; different organs could be exposed to higher or lower carbon nanotube concentrations for different time periods depending upon how the nanotubes are distributed within the organism and how rapidly excretion occurs. Previous biomedical studies indicated that organisms readily excrete injected modified nanotubes [62–64], but substantially different behaviors were observed for injected pristine SWNTs, with high masses remaining in the organisms 28 days after exposure [65]. The nanotubes tested by Folkmann et al. [61] were of high purity with regard to metal catalysts, which suggests that purification steps had occurred. Thus, these nanotubes may have acted more similarly to modified nanotubes and may be readily excreted and accordingly have a short residence time in the colon. It is also possible that DNA repair enzymes were stimulated in the colon mucosa cells and any potential damage that had occurred was repaired by the conclusion of the 24-h exposure period. Similarly, decreased DNA damage was detected in mice exposed to fullerenes by intratracheal instillation after 24 h compared with 3 h, which was speculated due to DNA repair [49]. In a separate in vivo study on carbon nanotubes, mice were exposed by intratracheal instillation [48]. Although exposure through oral gavage is intended to simulate toxicity after ingestion of the NPs as would be expected for some biomedical applications, intratracheal exposures are designed to test the potential impact of carbon nanotubes on organisms after inhalation. This exposure route could be an important risk for workers involved in nanomaterial manufacturing given the concern that carbon nanotubes may behave similarly to asbestos after inhalation [53, 57, 58]. Again, significantly elevated levels of SSBs were detected 3 h after the exposure using the alkaline comet assay. All together, these results suggest that DNA damage is a distinct possibility for organisms exposed to SWNTs. Although the potential of carbon nanotubes to induce oxidative damage to DNA in ecological receptors has not yet been investigated, past research indicates limited absorption and systemic distribution of carbon nanotubes after oral ingestion, whereas significant nanotube masses have been measured in organism guts [66–71]. Thus, in vivo ecological studies should focus, when possible, on DNA damage in gut tracts, where nanotube exposure is expected to be highest.

Carbon nanotubes have been shown to confound many common toxicity assays such as the 3-(4,5-dimethylthiazol-2-yl)-2,5-diphenyltetrazolium bromide assay [72]. As such, investigators are encouraged to confirm cytotoxicity and DNA damage end points through complementary methods when possible. A related approach is to test cells immediately after nanotube exposure using these assays. Large observed differences between control samples without nanotubes and those exposed to nanotubes only briefly would indicate an artifact that may impact results for longer nanotube exposure times. As will be discussed later for germanium NPs (GeNPs), a significant increase in apparent oxidative damage to DNA was observed for GeNPs when the cells were harvested immediately after introduction of the GeNPs [73].

Mechanistically, both the presence of low-level transition and heavy metal impurities within the SWNTs and the inherent biopersistence of the SWNT inside cells contribute to increased oxidative stress by the formation of ROS such as •OH, $O_2^{\bullet-}$, and H_2O_2 [20, 54]. These mechanisms are supported by the fact that even when SWNT agglomeration occurs, ROS production is suppressed but still ongoing [20]. When transition and heavy metals are chelated, ROS formation is measurably suppressed but the presence of the nanotubes continues to stimulate ROS production [54]. The •OH radical is known to be the predominant free radical that attacks DNA, but none of the studies investigated or reported on this phenomenon [7]. The reported mechanism of MWNT induction of DNA damage in vitro is similar to the mechanism ascribed to SWNTs. Oxidative damage to DNA involves the combined effects of low-level transition metal impurities acting as catalysts of the Fenton or Haber–Weiss reactions (producing •OH which can directly attack DNA) and the effects on persistent oxidative stress (and persistent ROS production) when cells try to ingest MWNT that are too large to fit inside, a phenomenon known as “frustrated phagocytosis” [74].

C_{60} fullerenes

The potential for fullerenes to induce oxidative damage to DNA has been studied less thoroughly than for carbon nanotubes, with fewer than half as many papers on the subject. Overall, the potential for fullerenes to damage DNA was generally equal to or less than that of similar masses of SWNTs. In in vitro experiments utilizing the alkaline comet assay, fullerenes induced SSBs in human lymphocytes at concentrations as low as 2 μg/mL [75], but did not induce SSBs without the addition of Fpg in a second study with mouse lung epithelial cells using a concentration of 100 μg/mL [20]. The source of this discrepancy is unclear and may result from the different dispersion techniques or sensitivities of the cell lines. Both SWNTs and C_{60} induced significant increases in the number of Fpg sites but not in the number

of strand breaks after the epithelial lung cells had been exposed for 3 h [20].

In an in vivo study that compared SWNTs and fullerenes, rats did not show elevated levels of SSBs after fullerenes had been introduced via intratracheal installation, whereas SWNTs did significantly damage the rat DNA [48]. Additionally, fullerenes only induced a significant increase in the 8-OH-dG levels in rat lungs after oral gavage at the highest dose (0.64 mg/kg), whereas SWNTs also caused an effect at a lower does (0.064 mg/kg) [61]. At this point, a mechanistic understanding of the cause of fullerene and SWNT toxicity is not available, and it is difficult to discern why different results are exhibited in experiments. The in vivo toxicity of fullerenes appears to relate to how the organisms are exposed to the NPs. Exposure by oral gavage yielded increased levels of 8-OH-dG at the higher-exposure concentration (0.64 mg/kg) but not the lower concentration (0.064 mg/kg) [61], whereas intratracheal installation of 0.2 mg per animal but not 0.05 mg per animal yielded a toxic response [48, 49]. In the study by Jacobsen et al. [48], the average mass of the mice was 18.5 g±1.4 g (N. Jacobsen, personal communication, 2010), which indicates that the fullerene concentration added which did not induce DNA damage was approximately 3 mg/kg. This value is much higher than that found by Folkmann et al. [61] (0.64 mg/kg), but given the numerous differences between these two studies, the source of the discrepancy is not clear.

Similarly to carbon nanotubes, fullerenes are very insoluble in water ($k_{ow}=10^{-6.67}$) and organisms will likely only be exposed to aggregates of these materials [76]. Research has shown that the experimental approach used to make fullerene aggregates can profoundly impact the observed toxicity. For example, Dhawan et al. [75] found that aggregates prepared using an ethanol solvent exchange resulted in fewer SSBs as measured by the alkaline comet assay than those produced via stirring in water. It is not clear at this point whether this difference stems from differences in the morphology of the NP aggregates or whether the solvent-exchange process could change the surface characteristics of the NPs, yielding decreased toxicity. Although none of the studies on DNA damage by fullerenes utilized fullerenes dispersed using tetrahydrofuran (THF), a number of other studies have indicated that this process can yield artificially high toxicity [77–79]. Observed toxicity was attributable to by-products from the THF procedure such as γ-butyrolactone and not the fullerene particles [77]. These findings highlight the importance of rigorously testing for artifacts caused by the material suspension procedures. Additionally, this research suggests that care should be taken in choosing the dispersion method, and that relevance to manufacturing processes or processes to which fullerenes would likely be exposed to in the natural environment or after biological uptake should be considered. If manufacturers typically use THF to disperse fullerenes for consumer products, research to date has yielded some important concerns related to the toxicity of this approach. But if this approach is not broadly used by industry, significant effort has been spent trying to understand toxicity results borne from an artifact related to the THF dispersion process.

The biochemical mechanism of fullerene-induced oxidative damage to DNA has not been thoroughly investigated. However, previous research has shown that C_{60} fullerenes are photosensitive compounds that are easily excited to the triplet state via visible or UV light [80–84]. The fullerene triplet state then undergoes an energy transfer to molecular oxygen to form singlet oxygen ($^1O_2$). The $^1O_2$ can then attack DNA directly and generate base lesions (preferentially at guanine) if the fullerene is inside the nucleus near the DNA [83]. Alternatively, and more likely, the very unstable $^1O_2$ will attack cytoplasmic or nuclear membrane lipids and form lipid peroxide radicals, which are known to preferentially attack guanine residues and generate guanine radical cations [80, 82]. The continued presence (biopersistence) of C_{60} fullerenes in the cell can contribute to the further oxidation of 8-OH-dG to form ALS, which can result in SSBs [80]. The detection of C_{60} fullerene-induced SSBs and oxidatively induced base damage at purine bases in the two reported studies supports the probability of the presented mechanism.

Carbon nanofibers

Firm conclusions about the potential for manufactured graphitic NPs to induce oxidative damage to DNA cannot be drawn at this point because only two relevant studies have been conducted [52, 85]. One study using cellulose-derived nanofibers showed no toxicity to Chinese hamster ovary cells even at the high concentration of 1 mg/mL [85], but commercially available graphitic nanofibers induced DNA damage at 3.8 μg/mL after 24 h [52]. The graphitic nanofibers did have a substantial concentration of metal catalyst remaining (4%), and this may partly account for the toxic response. Previous studies have found that metals leached from carbon nanotubes may cause substantial toxicity [59], and we recommend that this potential be tested in future studies. The mechanisms behind the observed DNA damage after carbon nanofiber exposure were not investigated [52].

Metallic nanomaterials

Metallic ENs have been manufactured in a variety of structural formats (rods, fibers, particles, cubes, stars, etc.), but so far, the capacity of the metallic ENs to induce

oxidative damage to DNA has only been investigated on particulate structures. This section will cover the current reports on cobalt, copper, gold, iron, nickel, platinum, silver, and mixed-composition particulate ENs.

Cobalt nanoparticles

Cobalt NPs (CoNPs) were shown to induce SSBs in human peripheral leukocytes and mouse fibroblast cells using the alkaline comet assay [86, 87]. Although cobalt ions did not induce a significant increase in the level of SSBs for the leukocytes [86], they caused similar but slightly fewer SSBs at similar cobalt concentrations compared with CoNPs for mouse fibroblast cells. These results indicate that the CoNP toxicity cannot be explained solely by toxicity of the cobalt ions. The discrepancy between the relative toxicity of the cobalt ions between these two studies likely stems from differences in the cell types and their resistance to DNA damage given that leukocytes were exposed to higher cobalt ion concentrations. Although the overall toxic impact on organisms as a result of NP exposure would not change based upon the source of those effects (ions or NPs), making this distinction is important. It has been postulated that there may be nanosize toxicity effects that may stem from the unique size, high surface area, and enhanced reactivity of NPs [88, 89]. Elucidating the extent to which NPs have these effects is critical from a risk assessment perspective. If different effects are not observed between nanoscale particles and dissolved ions of the same composition, new guidelines or regulations specific to NPs are likely unnecessary; as such, Table S1 indicates the studies that included investigations of the genotoxic effects of NPs and dissolved metal ions of the same element(s). Uptake of CoNPs by both leukocytes and fibroblasts was found to be approximately 2 orders of magnitude larger than that of cobalt ions [86, 87]. It is possible that CoNPs released significant quantities of cobalt ions within the cells, which could be the source of the observed toxicity. Future experiments utilizing X-ray absorption spectroscopy or transmission electron microscopy with electron energy loss spectroscopy could potentially be utilized to determine the speciation of the cobalt within the cells to gain a better mechanistic understanding of CoNP toxicity.

Cobalt–chromium nanoparticles

The potential for cobalt–chromium (CoCr) NPs and microparticles to induce oxidative damage to DNA has been investigated in two in vitro experiments using human fibroblasts. The comparison between NPs and micron-sized particles is important for risk assessment, because new regulations may be necessary for NPs if these smaller particles are found to pose novel or exacerbated risks compared with larger particles of the same chemical composition. The studies that compared NPs with larger particles are highlighted in Table S1. CoCr NPs induced significantly higher levels of SSBs as determined by the alkaline comet assay at concentrations of 3.85×10^{-1}, 3.85, and 3.85×10^{1} mg/mL as compared with the microparticles after 24 h of exposure [90]. Although the addition of CoCr microparticles caused significantly greater DNA damage than the NPs after 72 h at concentrations of 3.85×10^{-6}, 3.85×10^{-5}, and 3.85×10^{-1} mg/mL, the DNA damage levels for the NPs at each of these concentrations was significantly less than that of the control, which is itself a surprising result, suggesting that the NPs may have mitigated DNA damage. This result may stem from DNA repair, given that lower mean lesion levels were observed after 3 days of exposure than after 1 day of exposure. Overall, there was not a clear nanosize-related toxicity effect, and neither NPs nor microparticles were shown to be possess consistently higher genotoxicity. Similarly, there was not a clear pattern in the relative DNA damage potential of NP and microparticulate CoCr for fibroblasts exposed through either direct exposure or indirectly by adding the NPs above an insert that contained a BeWo cell barrier [91]. Interestingly, indirect exposures at concentrations of 0.08 and 0.8 mg/mL for both kinds of particles induced significant SSBs as detected via the alkaline comet assay and DSBs as detected via the γ-H2AX assay compared with the control. This result suggests that indirect effects of NP exposure are an additional important consideration given that DNA damage was observed across a cell barrier.

A partial mechanism for oxidative damage to DNA was developed and tied to the confirmed cytoplasmic uptake of the NPs, the subsequent intracellular corrosion of the NPs, and the final uptake of the predominant corrosion product, cobalt, but not the NPs themselves, into the nucleus [90]. In addition, chromium was found in the cytoplasm and nucleus, but at much lower levels. Cobalt ions (Co^{2+}) are known to bind to DNA, induce DNA–protein cross-links and SSBs, and inhibit DNA repair [92, 93]. Regarding the SSBs and 8-OH-dG detected in this study, it is likely that the high concentration of Co^{2+} in the nucleus, in the presence of H_2O_2, catalyzed a Fenton-like reaction and produced •OH which attacked the DNA directly. The second reported study described a mechanism by which the CoCr NPs generate oxidatively induced DNA damage based not on specific ROS-inducing qualities of the NPs themselves but on the NPs' ability to activate intracellular signaling pathways that indirectly lead to DNA damage [91]. The experimentally derived mechanism of oxidatively induced DNA damage demonstrated that NPs in contact

with a cellular wall or barrier can, just by their presence (no metal ions need cross the barrier), mediate the release of ATP. ATP can readily cross critical connexin gap junctions in the barrier, bind to P2 receptors on cells on the other side of the barrier, and induce oxidative damage to DNA (SSBs and DSBs). Further study of this mechanism is needed to understand why the presence of the CoCr NPs induces the release of ATP.

Copper nanoparticles

In the only study on copper NPs (CuNPs), CuNPs but not released Cu^{2+} ions or copper microparticles induced SSBs as determined using the alkaline comet assay and epithelial cells at a concentration of 80 μg/mL [94]. However, this concentration of CuNPs was highly cytotoxic, which suggests that the detected DNA damage may be partly a result of cell death and subsequent DNA fragmentation [12, 15]. Nevertheless, these results for CuNPs appear to represent a nanosize toxic effect for the CuNPs. The authors did not provide any information pertaining to the mechanism of DNA damage induction, other than stating that metal NPs can more easily pass through cell membranes compared to metal ions (i.e., Cu^{2+}).

Gold nanoparticles

Gold is the most electronegative metal (2.54 on the Pauling scale) and a difficult metal to oxidize. By most practical measures, gold is considered inert. The established view is that gold NPs (AuNPs) should also be nontoxic (disruptive to cellular integrity or viability) and nongenotoxic [95–100]. However, if AuNPs are sufficiently small (less than 2 nm) [101] or if AuNPs can be conjugated with specific nuclear receptors [102], the particles can indeed enter the nucleus and interact directly with DNA and/or chromosomes and induce toxicity and perhaps oxidative damage to DNA. The potential for AuNPs to induce DNA damage is currently unclear given the conflicting results described in the literature. There was no increase in the level of SSBs as determined by the alkaline comet assay after 0.54 μg AuNPs had been administered via intratracheal installation to mice [48]. This result suggests that inhalation risks of AuNPs at this concentration are limited. However, three in vitro studies on AuNP-induced oxidative damage to DNA suggest that AuNPs are not so harmless [103–105]. The studies involved the use of either citrate-stabilized or pegylated AuNPs to maintain the solubility and dispersibility of the NPs. Elevated levels of 8-OH-dG were observed in lung fibroblasts after exposure to 20-nm AuNPs at a concentration of 1 nM but not at 0.5 nM (50–100 and 25–50 μg/mL, respectively; personal communication) [105]. Kang et al. [104] showed that NP size may play an important role in the potential of NPs to induce DNA damage. AuNPs of 100- and 200-nm size resulted in elevated levels of SSBs as determined by the alkaline comet assay at concentrations of 25, 50, and 100 μg/mL, whereas 4- and 15-nm NPs did not have an effect at those same concentrations. AuNPs were also shown to induce SSBs via the alkaline comet assay with human monocytes exposed at an air–tissue interface [103]. Given the substantially different but important exposure conditions used in this study, it is difficult to compare these toxicity results with those obtained by the other studies. Overall, it appears that high AuNP concentrations on the order of 50 μg/mL and higher may have the potential to induce DNA damage. One important related factor that has been studied to a significant extent is uptake of AuNPs by cells. Li et al. [105] indicated that their 20-nm AuNPs were in vesicles clustered around the nucleus and Chithrani et al. [106] also indicated that 14-, 50-, and 74-nm AuNPs did not enter the nucleus. The rates at which AuNPs enter and exit cells is likely an important factor and one that has been shown to vary depending on the size and morphology of AuNPs [106, 107]. Relating accumulation rates and distribution within cells to toxicity results may help yield a clearer understanding of AuNP risks.

Iron nanoparticles

One study has been conducted on the potential for iron NPs (FeNPs) to induce oxidative damage to DNA [103]. FeNPs were shown to generate significantly increased levels of SSBs in human monocytes at an air–tissue interface using the alkaline comet assay at concentrations of 5.1 and 10.2 μg/cm^2; dose-dependent effects were observed [103]. The authors did not provide any information pertaining to the mechanism of DNA damage induction.

Nickel nanoparticles

One study has been conducted on the potential for nickel NPs (NiNPs) to induce oxidative damage to DNA [108]. NiNPs induced substantial damage to plasmid DNA as determined by agarose gel electrophoresis [108]. No additional information on the mechanisms of the DNA damage was provided.

Platinum nanoparticles

In the only in vitro study on platinum NPs (PtNPs), it was surprising that a dose–response relationship was not observed for SSB lesions via the alkaline comet assay and that only concentrations in the middle of the concentration range tested (0.1 and 1 ng/cm^2) caused significant increases in the numbers of SSBs as measured by the alkaline comet

assay [109]. This could stem from increased agglomeration at higher NP concentrations. This highlights one of the major challenges of nanotoxicology, namely, that NPs in solution may have different characteristics depending on the NP concentration. Oxidatively modified purine base lesions were also detected via the Fpg-modified comet assay [109].

Investigations into the mechanism for the oxidative damage to DNA resulted in the authors finding no significant evidence of oxidative stress, i.e., no intracellular ROS, even though PtNPs entered the cells. On the basis of this evidence and on preliminary evidence the report describes (but does not detail) demonstrating the formation of PtNP–DNA adducts, a tentative mechanism for PtNP-induced oxidative damage to DNA appears to involve the binding of PtNP directly to DNA. The Fpg-modified comet assay results tend to support this possibility since it is known that the Fpg not only repairs oxidatively induced purine lesions, but could also detect and repair nonbulky (e.g., methylated) purine adducts [110]. The removal of the PtNP–DNA adducts by the action of the Fpg during the comet assay could have led to the formation of the observed SSBs.

Silver nanoparticles

Silver NPs (AgNPs) in aqueous solutions slowly release silver ions (Ag^+) over time and these ions may account for the observed toxic effects [111]. Therefore, the intact AgNP and/or the released Ag^+ could theoretically interact directly with DNA if either of these species were able to cross the nuclear membrane and enter the nucleus. In fact, it has already been shown that Ag^+ forms stable complexes with DNA at N7 of purine bases [112]. Four studies have reported AgNP-induced oxidative damage to DNA using in vitro systems [103, 113–115]. Two of the studies [113, 115] reported detection of significant DSBs using the γ-H2AX assay and two studies [103, 114] reported detection of significant SSBs using the alkaline comet assay. AgNPs induced DSBs through H2AX phosphorylation even at concentrations as low as 1 μg/mL [115]. Importantly, Kim et al. [115] also tested the toxicity of $AgNO_3$ to assess the effects of the silver ions, which are known to be cytotoxic. In this study the toxicity caused by AgNPs and Ag^+ ions was similar on a silver concentration basis with regard to inducing DSBs, which suggests that AgNP leaching of silver ions was not fully responsible for the observed toxicity given that the NPs did not fully dissolve. The addition of antioxidant *N*-acetylcysteine prevented DSBs, thus suggesting that oxidative stress was the cause of the DNA damage. AgNPs were also shown to induce SSBs via the alkaline comet assay with lung fibroblast (IMR-90) and human cancer (U251) cells at concentrations of 25 and 50 μg/mL and higher, respectively [114]. The extent to which these effects were caused by dissolution of silver ions was not tested, and investigating such effects is strongly encouraged for future studies. In contrast to the four in vitro studies, the single in vivo study based on the use of chicken embryos reported the absence of AgNP-induced oxidative damage to DNA. No significant increases in the level of 8-OH-dG were detected via the LC/UV/EC method after introduction of 0.3 mL of a colloidal solution of 50 μg/mL Ag, Ag/Cu, or Ag/Pd NPs into the embryos [116].

Three out of four in vitro studies positively confirmed uptake of the AgNPs into the cytoplasm [113–115] and two of those confirmed the uptake of AgNPs into the nucleus [114, 115]. One study confirmed uptake of AgNPs into the cytoplasm, mitochondria, and nucleus [114] and the group conducting this study, in addition to Kim et al. [115], performed detailed mechanistic investigations into the cause of the AgNP-induced oxidative damage to DNA. What is most interesting about this set of studies on AgNPs is the fact that significant DSB lesions were reported in half of the studies; DSB lesions are difficult to repair and the most biologically significant DNA lesions, which suggests that AgNPs might possess a broad genotoxic potential. The mechanism for AgNP-induced oxidative damage to DNA, according to these reports, appears to be clearly associated with the presence of AgNP-induced ROS in the cytoplasm ($O_2^{\bullet-}$ and H_2O_2) [114, 115] in combination with the presence of structural damage to the mitochondria which led to interruption in the mitochondrial electron transport chain and production of additional ROS [114]. The use of AgNP dosing solutions in which all of the Ag^+ had been removed still induced oxidative damage to DNA, indicating that Ag^+ was not the major agent of ROS generation [114]. Disruption of the mitochondrial electron transport chain interrupts ATP synthesis and induces the formation of $O_2^{\bullet-}$. The $O_2^{\bullet-}$ subsequently dismutates to H_2O_2, which is freely diffusible throughout the cell and can readily pass through the nuclear membrane and enter the nucleus. Once in the nucleus, the H_2O_2 can undergo the Fenton reaction catalyzed by Cu^+ or Fe^{2+} ions adsorbed to DNA [117, 118].

Metalloid nanomaterials

Studies on oxidatively induced DNA damage with metalloid ENs have been conducted using both the amorphous and crystalline forms of particulate silica (SiO_2) and with GeNPs.

Silica nanoparticles

Amorphous silica is an FDA-approved food additive, whereas crystalline silica is a suspected human carcinogen and is involved in the pathogenesis of silicosis [119]. Previous researchers have shown that SiO_2 NPs are able to enter the nucleus [120] and that these NPs do not form ROS

in either cellular or acellular systems [121]. Two recent in vitro studies using amorphous SiO_2 NPs [122, 123] and one in vitro study using crystalline SiO_2 NPs [124] showed that SiO_2 NPs do not induce oxidative damage to DNA. On the other hand, two other in vitro studies demonstrated that SiO_2 NPs could induce oxidative damage to DNA [44, 46]. For the three SiO_2 NP studies in which DNA damage was not detected, mouse embryo fibroblast cells were exposed to a maximum NP concentration of 40 μg/mL [122], human lung epithelial cells were exposed to a maximum NP concentration of 500 μg/mL [123], and human B-cell lymphoblastoid cells were exposed to a maximum NP concentration of 120 μg/mL [124]. These studies all reported the absence of NP-induced oxidative DNA damage utilizing the alkaline comet assay to test for significant SSB lesions [122–124]; one of these studies also specifically tested for oxidatively induced base lesions using an 8-OH-dG antibody assay and found no accumulation of 8-OH-dG [123]. In contrast to the previous studies, a study based on a human carcinoma intestinal cell model established that SiO_2 NPs could induce oxidative damage to DNA [44]. This study utilized the Fpg-modified comet assay to test for SSBs due to the accumulation of oxidatively induced purine base lesions and found evidence of significant SSBs, but the SSBs may have been due to the use of NP concentrations (133.3 μg/mL) that were cytotoxic to the cells [44]. A final in vitro study reported the detection of significant SSBs using the alkaline comet assay [46]. This study utilized mouse embryo fibroblasts and NP concentrations of 5 and 10 μg/mL [46]. The initial mechanism of the detected DNA damage was reported to be due to oxidative stress (glutathione depletion, superoxide dismutase inhibition, lipid peroxidation) and intracellular formation of ROS, but no other mechanistic details were investigated or given. The only reported study regarding in vivo effects of SiO_2 NPs was performed using the aquatic organisms *Daphnia magna* and *Chironomus riparius*. The NPs did not induce significant SSBs as measured using the alkaline comet assay in either organism at a concentration of 1 μg/mL [125]. The studies by Gerloff et al. [44] and Yang et al. [46] did not determine the concentration at which effects were not observed to occur to yield lowest observed effect concentrations, whereas Lee et al. [125] did not determine whether damage would be observed at higher concentrations. As such, it is impossible to assess whether these different results stem from the concentrations used or from different sensitivities of the cells or organisms to SiO_2 NPs.

Germanium nanoparticles

No in vivo studies and only one in vitro cellular study have been conducted on GeNP-induced oxidative damage to DNA [73]. This lone study reported the detection of significant SSBs using the alkaline comet assay. However the mechanism of SSB formation was determined not to be due to oxidative stress and the formation of ROS, but rather due to the binding of GeNPs directly to the DNA during the alkaline comet assay procedure. When cells were treated with 0.36 mg/mL of GeNPs and then immediately harvested, a significant increase in the numbers of SSBs was observed, but no change in DSB formation was observed using H2AX phosphorylation. The authors concluded that NP attachment directly to DNA during the assay procedure probably resulted in arbitrary DNA fragmentation. This suggests that GeNPs may cause some artifact in the alkaline comet assay. In our opinion, researchers performing nanotoxicity studies should consider testing the apparent effects immediately after NP administration to ensure that the assay itself is not confounded by an unexpected characteristic of the NP. This artifact may also be limited to the alkaline comet assay, which suggests that complementary approaches should be considered to corroborate results if the comet assay is used.

Metal oxide nanomaterials

Metal oxide ENs exist mainly as particulate structures, but other structures do exist. This section reviews the current mechanisms of oxidative damage to DNA induced by particulate metal oxide structures based on aluminum, cerium, copper, iron, magnesium, titanium, zinc, and mixed metal oxide composites.

Aluminum oxide nanoparticles

One in vitro [126] and one in vivo [127] study (using rats) have been conducted on aluminum oxide (Al_2O_3) NP-induced oxidative damage to DNA. Both studies reported the detection of significant SSBs using the alkaline comet assay. The in vitro study on Al_2O_3 NPs tested mouse lymphoma cells and human bronchial epithelial cells with and without the addition of the S-9 metabolic activation system [126]. The mouse lymphoma cells showed significant SSBs in the presence of S-9 at all concentrations, whereas only at 2,500 μg/mL was a significant increase seen in the absence of S-9. However, significant SSBs were detected at all concentrations with and without S-9 for the human bronchial epithelial cells. The data thus suggest that adding S-9 increased the DNA damage to the cells, but a clear determination could not be made. In an in vivo study, rats were exposed to 500, 1,000, or 2,000 mg/kg of 30- or 40-nm NPs or microparticles by oral gavage to simulate risks as a result of ingestion exposure [127]. The 30- and 40-nm NPs generally exhibited the same potential for inducing SSB lesions, with increased damage observed for

1,000 and 2,000 mg/kg after 4 and 24 h. However, no significant SSBs were observed after exposing the rats to 500 mg/kg of the NPs or microparticles, thus suggesting this concentration to be a threshold below which these effects would not be expected. Additionally, the NPs did not induce the formation of SSBs at any of the concentrations after 72 h. This result and the trend for decreased DNA comet tail percentages with increased time suggest that the rats have efficient repair enzymes to counteract the DNA damage effects of these concentrations of Al_2O_3 NPs or microparticles. It is also important to note that Al_2O_3 microparticles did not induce significant SSB lesions at any concentration or time point. The impact of Al^{3+} ions was not investigated nor was the rate at which dissolution occurred from the NPs or microparticles, which precludes drawing a conclusion that there was a NP effect beyond NP dissolution to ions. For both of these studies, it is important to note that the rats and cells were being exposed to very high Al_2O_3 NPs concentrations. In comparison, Folkmann et al. [61] exposed rats to a maximum carbon nanotube or fullerene dose of 0.64 mg/kg, a concentration that is almost 4 orders of magnitude less than the highest concentration used by Balasubramanyam et al. [127]. Similarly, the mouse lymphoma cells were exposed to very high NP concentrations ranging from 0.125 to 0.5% by mass of the cell medium, although the bronchial epithelial cells were exposed to concentrations 1 or 2 orders of magnitude smaller. In our opinion, this research highlights the importance of determining reasonable NP exposure estimates to guide the concentration ranges used in toxicology studies. Although significant effects may be observed at very high concentrations, they do not necessarily translate to these particles posing a significant risk to humans or ecological receptors if the maximum likely exposure concentration is several orders of magnitude smaller. However, the lack of an effect at these high concentrations would suggest the lack of an effect at a lower concentration, unless substantial particle aggregation masked the NP toxicity at the higher concentrations. And finally, neither Al_2O_3 NP study reported investigations or experimental results related to understanding the mechanisms behind the observed NP-induced damage to DNA.

Cerium oxide nanoparticles

Four studies (three in vitro and one in vivo) have been conducted on the induction of oxidative damage to DNA via cerium oxide (nanoceria; CeO_2) NPs [125, 128–130]. The genotoxicity of CeO_2 NPs to cells was shown to depend on the dose. Two in vitro cellular studies reported opposite outcomes using the alkaline comet assay: the study by Pierscionek et al. [128] did not report significant SSBs, whereas the study by Auffan et al. [130] reported the detection of significant SSBs due to the redox-cycling capability of CeO_2 NPs. Whereas Pierscionek et al. [128] did not find DNA damage to human lens epithelial cells at 5 or 10 μg/mL, Auffan et al. [130] consistently observed DNA damage to human fibroblasts at concentrations above 60 μg/mL; Auffan et al. [130] detected significant damage at 0.6 μg/mL but not at 0.006, 0.06, or 6 μg/mL, thus making it difficult to determine a specific concentration at which oxidative damage to DNA would not be expected to occur. Importantly, Auffan et al. also discovered that the DNA damage levels induced by CeO_2 NPs and microparticles were similar when compared on a surface area basis, but that CeO_2 NPs were significantly more toxic on a mass basis. The appropriate metric that should be used for comparing NPs and microparticles is currently unclear, and in our opinion, researchers are encouraged to include both surface area and mass to facilitate comparisons among studies. Another issue related to the dose metric involves whether to indicate cell exposure concentrations on a mass per volume or a mass per cell dish exposure area basis. Given that NPs often settle during the course of an experiment, Stone et al. [131] recommend using the mass per surface area as the more relevant metric, although providing the concentrations in both units is preferable to better enable comparisons among studies. In the third in vitro study, human lung A549 cells showed increased oxidative damage to DNA when they were exposed to CeO_2 NPs during a glovebox exposure setup intended to simulate exposure conditions near a CeO_2 NP production facility [129]. This study utilized antibody staining for 8-OH-G and found significant accumulation of the lesion [129]. However, the mechanism for the formation of 8-OH-G was not investigated or reported. Nevertheless, these results indicate that DNA damage risks to workers should be taken seriously for CeO_2 NP production. In one of the very few studies on the DNA damage risks to ecological organisms, Lee et al. [125] showed that 15- and 30-nm CeO_2 NPs could damage the DNA of *Chironomus riparius*, whereas 15-nm NPs but not 30-nm NPs damaged the DNA of *Daphnia magna*; the resulting data using the alkaline comet assay showed significant formation of SSB lesions, but the mechanism of lesion formation was not investigated [125]. The cause for this discrepancy in the *Daphnia magna* data between the two different NP sizes was not determined. But, DNA damage results correlated with mortality observed for the two organisms; there was a statistically significant increase in *Daphnia magna* mortality with only the 15-nm NPs and in *Chironomus riparius* mortality with both sizes. As such, additional research is needed to elucidate the mechanisms through which CeO_2 NPs induce oxidative damage to DNA.

Copper oxide nanoparticles

Three studies on CuO NP-induced DNA damage in in vitro cellular models have been conducted [22, 23, 94]. All three studies reported detection of significant SSB lesions using the alkaline comet assay and two of the studies specifically applied the Fpg-modified comet assay to detect significant SSBs due to the accumulation of oxidatively modified purine lesions [22, 23]. Interestingly, all three studies noted significant oxidative damage to DNA at NP concentrations of 80 μg/mL and in each case the DNA damaging effects of CuO NPs were stronger than the DNA damaging effects of CuO micron-sized particles. In all studies, CuO NPs were consistently and substantially more cytotoxic and induced significantly more oxidative damage to DNA than added Cu^{2+} ions or Cu^{2+} ions released from the CuO NPs themselves. Surprisingly, the Cu^{2+} ions released from CuO NPs were more cytotoxic than the added Cu^{2+} ions, but the released Cu^{2+} ions did not induce significant oxidative damage to DNA. On the basis of conclusions from all of the studies, the mechanisms behind the induction of DNA damage are not clear, but it is apparent that released Cu^{2+} ions are not the causative factor for the in vitro oxidative stress and the resulting DNA damage. On the other hand, it is clear that CuO NPs do induce oxidative stress. A recent study has shown that CuO NPs engage in redox cycling, produce sustained high levels of ROS, and alter antioxidant enzyme (catalase, glutathione peroxidase) activity [132]. On the basis of this evidence, two potential mechanisms of CuO NP-induced DNA damage emerge. Because it is known that metal ions are not generally effective at penetrating the cell membrane, but metal NPs and some metal oxides such as CuO enter cells at significant rates, [121, 132], it is possible that CuO NPs enter the cell and are taken up into lysosomes. The acidic environment of the lysosomes then causes CuO NP degradation into Cu^{2+} ions, which are released into the cytoplasm and are subsequently reduced by $O_2^{\bullet-}$ to Cu^{+} ions [132]. The Cu^{+} ions can then catalyze the formation of •OH by reacting with H_2O_2; the •OH generated can then attack DNA if it is generated near the DNA in the nucleus. The other potential mechanism of CuO NP-induced DNA damage is based on CuO NPs directly entering the cell and interacting with mitochondria and inducing mitochondrial depolarization [23]. Mitochondrial depolarization results in loss of mitochondrial membrane potential, disruption of the electron transport chain, and the release of ROS into the cytoplasm. Although there are no in vivo studies on CuO NP-induced DNA damage, our laboratory is currently investigating the mechanisms of CuO NP-induced DNA damage in plants using GC/MS.

Iron oxide nanoparticles

Iron oxides exist in numerous structural forms but only three nanoparticulate forms have been investigated for their ability to induce oxidative damage to DNA in in vitro cellular models: γ-Fe_2O_3 NPs (maghemite, contains Fe^{3+}), Fe_2O_3 NPs (hematite, contains Fe^{3+}), and Fe_3O_4 NPs (magnetite, contains both Fe^{2+} and Fe^{3+}). Only one study has been conducted using γ-Fe_2O_3 NPs and the authors reported the absence of significant SSB lesions using the alkaline comet assay [133]. This study was performed using human fibroblasts at a maximum NP concentration of 100 μg/mL. Three studies [22, 23, 134] have been conducted on Fe_2O_3 NPs and two of the studies [22, 23] reported the absence of significant SSB lesions using both the alkaline comet assay and the Fpg-modified comet assay. The studies that reported the absence of significant SSB lesions were conducted on human lung epithelial cells using maximum Fe_2O_3 NP concentrations of 80 μg/mL. However, the remaining Fe_2O_3 NP study did report the detection of significant SSB lesions using the alkaline comet assay, but no accumulation of 8-OH-dG using ELISA [134]. In this study, Fe_2O_3 NP-induced oxidative damage to DNA in human diploid fibroblasts at concentrations of 50 and 250 μg/mL and in human bronchial epithelial cells at 250 μg/mL. These overall results suggest that the risks of DNA damage from Fe_2O_3 NPs appear to be minimal except at very high concentrations. Thus γ-Fe_2O_3 NPs and Fe_2O_3 NPs, both of which consist of Fe^{3+} ions, do not appear to generally promote oxidative damage to DNA in in vitro models. It seems probable, on the basis of acellular ROS-induction experiments performed in the study that did report Fe_2O_3 NP-induced SSB lesions, that iron oxide NPs that consist of Fe^{3+} ions are unable to easily generate ROS in vitro [134]. The established mechanism of ROS production from iron requires the reduction of Fe^{3+} to Fe^{2+} for Fe^{2+} ions to catalyze the Fenton reaction and produce •OH, which can attack DNA if the •OH is near the DNA. The reduction of Fe^{3+} to Fe^{2+} is not easily achieved under normal physiological conditions and requires special reducing agents or a reducing environment in the cell for the reduction to occur [132, 135]. This likely explains why γ-Fe_2O_3 NPs and Fe_2O_3 NPs do not generally induce in vitro oxidative damage to DNA. On the other hand, Fe_3O_4 NPs did induce the formation of SSBs in two separate studies [22, 23]. These authors utilized the Fpg-modified comet assay to detect significant SSBs due to the accumulation of oxidatively modified purine base lesions. Lesion accumulation was only observed at high (80 μg/mL) NP concentrations. This result was not surprising because Fe_3O_4 NPs contain both Fe^{2+} and Fe^{3+} ions. However, the studies did not investigate or describe any potential mechanisms for the observed oxidative damage to DNA.

There have been no studies investigating or reporting on the in vivo effects of any of the iron oxide NPs thus far.

Magnesium oxide nanoparticles

In the lone study on the effects of magnesium oxide (MgO) NPs, no significant increase in the numbers of SSBs was detected in a Caco-2 cell model utilizing both the alkaline comet assay and the Fpg-modified comet assay [44]. This study utilized NP concentrations as high as 133.3 μg/mL. Additional research is needed using lower concentrations to yield more definitive information about the potential for MgO NPs to induce DNA damage should MgO NPs become widely used in consumer goods.

Titanium dioxide nanoparticles

Titanium dioxide (TiO_2) NPs are semiconductors and have been shown to be strongly photoactive in in vitro cell models [136]. These NPs are perhaps the most challenging NPs to study with regard to their potential genotoxic effects, because in addition to the typical NP challenges related to different sizes and aggregation states, TiO_2 NPs exist in two different crystalline forms (anatase and rutile) and are photoactive. The widespread interest in the risks of TiO_2 NPs is in large part a result of the frequency with which they are already being used in commercial products. The estimated concentrations of these particles being released into the environment are typically orders of magnitude larger than those for any other NPs [137, 138].

The induction of oxidative damage to DNA by TiO_2 NPs is thought to stem from their inherent photoactivity and ROS generation potential. The ROS generated are initially formed on the surface of the NPs, but when released, the ROS are able to freely diffuse throughout the cellular matrix. However, numerous in vitro studies have demonstrated oxidative damage to DNA induced by TiO_2 NPs both in the presence of UV irradiation and/or simulated sunlight [136, 139–147] and in the absence of UV irradiation [19, 22, 23, 44, 134, 142, 143, 146, 148–150]. In two studies using fish cells, TiO_2 NPs in the absence of irradiation were found to cause an increase in oxidized purine base lesions in one study but not in the other study [142, 144]. TiO_2 NPs generated oxidatively modified DNA lesions (detected via the Fpg-modified comet assay, but not with the Nth-modified comet assay) in the absence of UVA irradiation at concentrations of 1, 10, and 100 μg/mL using goldfish skin cells [142]. In the absence of either BER enzyme, significant damage was only observed at 100 μg/mL TiO_2 NPs. For rainbow trout gonad cells treated with TiO_2 NPs in the absence of UVA irradiation, a similar increase in the number of oxidative lesions was not observed with the Fpg-modified comet assay at concentrations of 5 and 50 μg/mL [144]. These results suggest that TiO_2 NPs in the absence of UVA irradiation may selectively impact Fpg-sensitive sites, but the results are inconclusive. In the presence of UVA irradiation, significant oxidative damage to DNA was detected under almost all conditions for these studies. This highlights the importance of determining whether organisms exposed to TiO_2 NPs accumulate the NPs in a location (e.g., the skin) were UV light could potentially interact with the NPs. No effects from TiO_2 NPs were observed in the absence of irradiation after exposing human diploid fibroblasts, human bronchial epithelial cells, human carcinoma intestinal cells, and human keratinocytes using the alkaline comet assay [44, 134, 143]. Conversely, TiO_2 NPs were observed to induce SSBs as measured by the alkaline comet assay in the absence of UV irradiation in human sperm and lymphocyte cells and bronchial epithelial cells [19, 146]. Increases in 8-OH-dG levels were also detected for human diploid cells in the absence of UV irradiation [134]. Different NP doses cannot explain the difference in these results given that a concentration of 3.73 μg/mL induced SSBs in human sperm and lymphocytes [146], whereas concentration of 250 μg/mL did not induce significant increases in the level of SSBs as measured by the alkaline comet assay [134]. Additionally, both of these studies used anatase TiO_2 NPs, thus indicating that the type of TiO_2 used cannot account for the difference. Although some of these differences may be due to use of different cell lines, these results also highlight one of the major weaknesses of the alkaline comet assay—that it is a nonspecific assay that includes many different lesions as one aggregate measurement. Having a more clear indication of the various types of lesions affected by nanoparticulate TiO_2 could likely lead to insights about how DNA damage occurs and why so many of the past studies gave apparently conflicting results.

Additionally, there is one important potential artifact for TiO_2 NPs that should be considered, especially in studies utilizing the alkaline comet assay. Gerloff et al. [44] did not detect an increase in the level of SSBs when the slides for the alkaline comet assay were prepared in the dark, but they did detect significant SSBs when the slides were prepared under normal laboratory lighting. In our opinion, unless researchers explicitly state that all handling steps were conducted in the dark, results for TiO_2 NPs using the alkaline comet assay should be viewed with caution. Even in the absence of UV irradiation, there is accumulated evidence (detection of intracellular ROS, inhibition of intracellular ROS by ROS scavengers, activation of oxidative stress markers, etc.) from reports that demonstrated the formation of oxidatively induced DNA lesions [19, 22, 23, 44, 134, 142, 146, 148–150]. This may be an artifact of laboratory lighting and/or of ambient lighting for some of the studies. Nevertheless, data

from all of the reported studies indicate that there exist two probable mechanisms of TiO_2 NP-induced oxidative damage to DNA. To derive these mechanisms, a variety of assays have been utilized to detect and measure the presence of significant SSB lesions and oxidatively modified purine base lesions, including the alkaline comet assay, Fpg-modified comet assay, plasmid nicking/agarose gel electrophoresis assay, 8-OH-dG antibody ELISA and LC/EC or LC/UV methods for 8-OH-dG [19, 22, 23, 44, 134, 136, 139–146, 148–150].

The first mechanism of TiO_2 NP-induced DNA damage, but not necessarily the primary mechanism, is based on the photoactivated (via appropriately energetic light) induction of electrons from the valence band of the TiO_2 NP to the conduction band [136]. This results in the formation of holes in the valence band and electrons in the conduction band. The hole and electron pairs can either recombine or diffuse rapidly to the surface of the NP. At this point, two distinct processes based on the diffusion of the holes and electrons to the surface of the NP occur: (1) the positively charged holes react with (oxidize) adsorbed water or hydroxyl ions on the surface of the NP to produce •OH and (2) the electrons react with (reduce) molecular oxygen to produce $O_2^{\bullet-}$. On the basis of the cellular uptake and presence of TiO_2 NPs in the cytoplasm, the short-lived •OH is unlikely to reach and enter the nucleus and attack DNA. On the other hand, $O_2^{\bullet-}$ can dismutate to H_2O_2, which is freely diffusible throughout the cell and can readily pass through the nuclear membrane. Once in the nucleus, the H_2O_2 can undergo the Fenton reaction catalyzed by Cu^+ or Fe^{2+} ions inherently adsorbed to DNA and produce the highly reactive •OH, which can directly attack DNA [117, 118]. The second mechanism of TiO_2 NP-induced oxidative damage to DNA is also based on the photoactivation of TiO_2 NP and the production of electron–holes pairs. The difference is that the transition metal ion Cu^{2+} (or potentially other transition metals), which is normally present in the cytoplasm, can be reduced to Cu^+ ion by the electron in the electron–hole pair or by the $O_2^{\bullet-}$ that is formed via the reduction of molecular oxygen [139]. The Cu^+ can then react with the H_2O_2 (or •OH) in the cytoplasm and produce copper peroxyl species which can readily diffuse through the nuclear membrane and attack DNA. The crystalline form of TiO_2 NPs, rutile or anatase, also mediates which DNA damage mechanism is predominant and which type of ROS is formed. Rutile TiO_2 NPs have been shown to produce mainly •OH and anatase TiO_2 NPs have been shown to produce $O_2^{\bullet-}$, H_2O_2, and peroxyl radicals [151]. Most recently, it was discovered that photoactivated TiO_2 NPs generate not only •OH and $O_2^{\bullet-}$ via the mechanisms previously described, but also generate carboxyl radical anions ($CO_2^{\bullet-}$) [152]. The $CO_2^{\bullet-}$ also reacts, similarly to the electron of the photogenerated electron–hole pairs, with adsorbed molecular oxygen on the particle surface to generate additional $O_2^{\bullet-}$, which can dismutate to H_2O_2 and diffuse to the nucleus.

Four in vivo studies have been conducted on TiO_2 NP-induced oxidative damage to DNA [108, 125, 153, 154]. Two studies reported the absence of oxidative damage to DNA [125, 153] and two studies reported the presence of oxidative damage to DNA [108, 154]. In one study that did not indicate DNA damage, rats were exposed to concentrations up to 1.2 mg TiO_2 per lung by intratracheal instillation and there was no detection of significant levels of 8-OH-dG using a polyclonal antibody staining assay and an immunohistochemical assay [153]. The second result indicating a lack of DNA damage was from a study of *Daphnia magna* and *Chironomus riparius*; no significant SSB lesions were detected using the alkaline comet assay [125]. However a recent study, based on the use of a mouse model and three different assays, reported the detection of significant SSB (alkaline comet assay), DSB (γ-H2AX assay), and oxidative purine base (LC/EC method for 8-OH-dG) lesions in mouse livers [154]. In this study, mice were exposed to TiO_2 NPs (50 mg/kg) via oral ingestion. The authors concluded that the DNA damage occurred because of persistent inflammation combined with severe oxidative stress due to the presence of the TiO_2 NPs in the mice. In the final study, rats were dosed (1 mg/mL) with TiO_2 NPs via intratracheal exposure and DNA strand breaks were detected using the plasmid nicking/agarose gel electrophoresis assay. Oxidative damage to DNA was detected, but the authors indicated that the damage was minimal [108].

Zinc oxide nanoparticles

The induction of oxidative damage to DNA by zinc oxide (ZnO) NPs was investigated in six different in vitro cellular systems [22, 44, 46, 146, 155, 156]. The concentration of ZnO NPs needed to cause toxicity varied among the different studies, with 2 and 40 μg/mL not causing DNA damage in one study [22], yet another study using the same cell line (A549) showed DNA damage at concentrations of 10, 12, and 14 μg/mL using NPs from the same manufacturer [155]. The discrepancy between these results may stem from the exposure duration given that the cells were exposed for either 4 h [22] or 24 h [155], respectively. These results suggest that the exposure duration may be a critical component for determining the extent to which ZnO NPs could induce DNA damage in human or ecological exposures. Determining the elimination rates of ZnO NPs in organisms is thus a high priority for research given that faster elimination causes shorter exposure durations. All studies on ZnO NPs used the alkaline comet assay to report the detection of significant SSBs. Two of the six studies [22, 44] also utilized the Fpg-modified comet assay and

reported the detection of additional SSBs due to the formation of ZnO NP-induced purine base lesions. These two studies showed that ZnO NPs can significantly increase the level of oxidatively induced lesions when high NP concentrations (80 μg/mL or higher) are utilized [22, 44]. Even though ZnO is a semiconductor [136], ZnO NPs do not appear to behave like TiO_2 NPs in the photogeneration of ROS, and Zn^{2+} is not a transition metal and is unlikely to catalyze the formation of ROS via the Fenton reaction in biological systems [46]. Two studies actually reported the detection of intracellular ROS [46, 155], but the authors could not or did not determine the source/type of the ROS. In addition, the levels of markers of oxidative stress were elevated in four studies [44, 46, 155, 156], but none of the reports investigated the mechanisms behind these findings. Even though excess oxidative stress appears to be a key step for the induction of oxidative damage to DNA by ZnO NPs, the exact DNA damage mechanism has not been established. There have been no studies investigating or reporting on the in vivo effects of ZnO NPs thus far. In summary, the observed oxidative damage to DNA at low NP concentrations (10 μg/mL or lower) [155, 156] indicates that a better understanding of the genotoxic risks of ZnO NPs should be a priority.

Mixed metal oxide composite nanoparticles

No in vivo studies and only one in vitro cellular study have been conducted on the potential for a mixed metal oxide composite NP ($CuZnFe_2O_4$ NP) to induce oxidative damage to DNA [22]. This lone study reported the detection of significant SSB lesions using both the alkaline comet assay and the Fpg-modified comet assay. There was not a discrete investigation into the mechanism of the NP-induced DNA damage, but the study report did note that $CuZnFe_2O_4$ NP (contains Fe^{2+}) generated significantly more DNA damage than iron oxide NPs (Fe_2O_3 NPs or Fe_3O_4 NPs). The authors did not speculate, but one could extrapolate that Fe^{2+} ions potentially released from $CuZnFe_2O_4$ NPs could catalyze Fenton chemistry in the nucleus and promote oxidative damage to DNA via the processes described earlier in this review.

Semiconductor quantum dots

Semiconductor quantum dots (Qdots) are usually composed of elements in periodic groups II–VI, III–V, or IV–VI, but so far the capacity of Qdots to induce oxidative damage to DNA has only been investigated with groups II–VI (IUPAC groups 12 and 16) elements. Determining the potential toxic effects of Qdots is a complex challenge as a result of the numerous compositions that can be synthesized with different cores, shells, and surface coatings, each of which may impact the toxicity. Additionally, Qdots are often synthesized using metals known to be toxic at sufficiently high concentrations such as selenium and cadmium. Thus, the toxicity of weathered Qdots, which release substantial concentrations of these ions, was found to be profoundly greater than that of intact Qdots [157]. The long-term risks of exposure to these materials are therefore intimately related to environmental or biological conditions that affect Qdot stability. This section will cover the current reports on cadmium selenide (CdSe) and cadmium telluride (CdTe) Qdots.

Cadmium selenide quantum dots

Three in vitro studies on CdSe Qdot-induced oxidative damage to DNA have been conducted, and all three studies utilized Qdots engineered with protective shells of zinc sulfide (ZnS) [158–160]. The first study reported the detection of significant SSB lesions induced by the CdSe–ZnS Qdots using the alkaline comet assay; however, it was eventually discovered that the Qdots were not the cause of the SSBs [159]. In this study, carboxylated Qdots (Qdots-COOH) but not Qdots-OH, Qdots-NH_2, Qdots-OH/COOH, or Qdots-NH_2/OH induced DNA damage in human lymphoma cells [159]. These authors found that purifying the Qdots-COOH substantially decreased their toxicity, and that comparable concentrations of some of the chemicals used during the Qdots synthesis for this study caused enhanced DNA damage. The oxidative damage to DNA was actually caused by the hydrophilic surface coating on the Qdots. These results suggest that manufacturers may be able to substantially reduce the potential toxicity of products containing Qdots by thoroughly purifying them prior to their incorporation in consumer goods. The second study reported the definitive detection of CdSe–ZnS Qdot-induced oxidative damage to DNA via the plasmid nicking/agarose gel electrophoresis assay; however, nicked DNA gel bands were not identified as due to SSB or DSB lesions, but just as damaged and undamaged bands [158]. This study also investigated the effect of UV irradiation or the lack thereof on DNA damage and the authors were able to formulate some mechanistic details regarding Qdot induction of DNA damage involving both photoactivated and surface-oxide-generated ROS, but not involving released Cd^{2+} (the ZnS shell inhibited the release of Cd^{2+} ions). The photoactivation of ROS was not a simple semiconductor photoinduction of ROS as is described for TiO_2 NPs because the ZnS shell can prevent the holes from the electron–hole pairs from reaching the surface of the Qdots and participating in oxidation reactions. So the only active participants in the creation of ROS (in the case of Qdots with protective shells) are photogenerated electrons which can reduce molecular oxygen and form $O_2^{\bullet-}$. The other mechanism put forth for the formation of ROS actually involves the ZnS protective shell and does not require

photogeneration. The ZnS shell can undergo a slow surface oxidative process in aqueous environments: sulfur forms sulfur dioxide (SO_2), which desorbs into solution and forms sulfoxide radical anion ($SO_2^{\bullet-}$). In the presence of air, $SO_2^{\bullet-}$ is oxidized to $O_2^{\bullet-}$ [161] and $O_2^{\bullet-}$ dismutates to •OH, which can oxidatively damage DNA. The study reported the generation of ROS when the Qdots were placed in the dark and reduced levels of oxidative damage to DNA (compared with the levels observed during photoactivation), but the identity of the ROS could not be ascertained. The final in vitro study also reported CdSe–ZnS Qdot-induced DNA damage under photoactivation via the use of the plasmid nicking/agarose gel electrophoresis assay [160]. DNA strand breaks were not observed when the Qdots were tested in the dark; thus, the mechanism of DNA damage was once again not related to the release of Cd^{2+} ions. The BER enzymes Fpg and Nth were also incorporated in the experiments and the observation of DNA strand breaks for both enzymes indicated that Qdots induced oxidative damage to DNA at both pyrimidine and purine base sites. A detailed mechanism for Qdot-induced oxidative damage to DNA was given in the report. Initially, Qdots are photoactivated and undergo a nonradiative energy transfer to molecular oxygen which induces the formation of $^1O_2$. The $^1O_2$ then forms •OH (the mechanism for this conversion was not given by the authors), which can attack DNA if the •OH is near the DNA in the nucleus. The authors of the study described two possible paths of oxidative attack on DNA that •OH might take: (1) abstraction of a hydrogen atom from a ribosyl group on DNA, thus creating ribosyl centered radicals—the ribose-centered radicals then cleave the ribose–phosphate backbone, which results in DNA strand breaks—and/or (2) direct addition of •OH at the C8 position of a guanine base (for example) to produce an N7-centered guanine radical which can subsequently rearrange to either 8-OH-dG or FapyGua depending on the redox microenvironment of the cell.

In summary, on the basis of the reported in vitro studies, it appears that CdSe–ZnS Qdot-induced DNA damage is mediated by either photogenerated ROS or by surface-oxide-generated ROS. Cadmium ions do not appear to have a significant role in inducing oxidative damage to DNA when Qdots are synthesized with a protective shell. Thus far, there have been no studies investigating or reporting on the in vivo effects of CdSe–ZnS Qdots related to the induction of oxidative damage to DNA.

Cadmium telluride quantum dots

Three studies on CdTe Qdot-induced DNA damage have been conducted, and all three studies utilized Qdots engineered without protective shells [48, 162, 163]. Not surprisingly, all three studies reported detection of DNA damage. The sole in vitro cell study utilized the alkaline DNA precipitation assay to detect significant DNA damage (strand breaks) in rainbow trout hepatocytes that were induced by CdTe Qdots, but the authors did not investigate nor report any DNA damage mechanisms [163]. The authors studied the effects of CdTe Qdots on the hepatocytes after the Qdots had been aged for 2 months or 2 years. Although significantly increased DNA damage was observed at concentrations as low as 0.4, 10, and 50 μg/mL for Qdots aged for 2 months, DNA damage was not observed at 2 or 250 μg/mL. This lack of a dose–response effect is surprising, and these results correlated with the labile zinc/cadmium, thus suggesting that dissolution of the Qdots played an important role in the observed toxicity. Results for the CdTe Qdots aged for 2 years also did not show a dose–response effect, but these results were not correlated with the labile zinc/cadmium. The cause of the DNA damage potential for these aged Qdots is unclear, and future studies that more vigorously characterize the aged Qdots are needed to unravel these effects. One in vivo ecotoxicology study using the alkaline DNA precipitation assay and a freshwater mussel (*Elliptio complanata)* model reported significant oxidative damage to DNA on the basis of an observed reduction in the number of DNA strand breaks [162]. The Qdots were found to induce DNA damage in the gills and digestive glands at low microgram per milliliter concentrations. Similar results were observed in the digestive glands but not the gills after exposure to 0.5 μg/mL Cd. This suggests that these Qdots may possess some unique toxicity to the gills. Another in vivo study using the alkaline comet assay and a mouse model also reported the detection of significant SSBs [48]. Positively and negatively charged CdTe Qdots induced DNA damage in mice lungs after intratracheal installation of a mass of Qdots with 63 μg Cd [48]. However neither in vivo study investigated nor reported any information on DNA damage mechanisms. The DNA damage results reported for CdTe Qdots without protective shells most likely were due to released Cd^{2+} ions. Cadmium(II) ions are taken up by calcium channels in plasma membranes and Cd^{2+} is known to inhibit DNA synthesis [160]. Cadmium ions are known to induce ROS (H_2O_2, $O_2^{\bullet-}$, •OH) [164, 165], to interact directly with the major groove of DNA, and to cause DNA damage [166, 167].

Conclusions

The following are a number of key conclusions/recommendations for future research on nanomaterial-induced oxidative damage to DNA:

1. The assays utilized to assess oxidative damage to DNA were often not sufficiently specific to allow for a thorough mechanistic understanding of how the DNA

damage was generated. The alkaline comet assay, in particular, combines a broad range of DNA lesions into a single measurement, yet this is the most commonly utilized assay. For future investigations, it is recommended that researchers consider using chromatography- and mass-spectrometry-based techniques, in parallel with the alkaline comet assay, to obtain more specific and more quantitative information on individual DNA lesions. However, researchers should be aware that chromatography-based techniques are not without certain drawbacks, not least of which is the possibility of artifactual formation/elevation the level of DNA lesions during sample preparation and analysis [168, 169]. For example, molecular oxygen is often present in buffers and solutions for preparing DNA samples for analysis and can result in artifactual lesion formation as has been previously demonstrated for 8-OH-dG [169]. To prevent the occurrence of such lesion artifacts before and during chromatographic analysis, researchers must adopt and utilize specialized sample preparation procedures.

2. The extent to which the nanomaterials were characterized in the reported studies varied greatly; some studies only provided characterization data obtained from the manufacturer (see Table S1). However, it is well known that manufacturer characterization data can be inaccurate and incomplete. Researchers are strongly encouraged to characterize each nanomaterial's physical, chemical, and electronic properties in their own laboratories using appropriately rigorous analytical techniques. Reliable nanomaterial characterization data will promote and accelerate better interlaboratory comparisons of genotoxicity data [3, 6, 43, 170].
3. Numerous potential experimental artifacts have been discussed throughout the review which can significantly impact the observed results. For example, GeNPs appeared to induce SSBs using the alkaline comet assay even when the cells were harvested at time zero [73]. Additionally, TiO_2 NPs appeared to induce SSBs using the alkaline comet assay when the slides were processed in normal room light but did not induce SSBs when the slides were processed in the dark [44]. There are also experimental artifacts related to synthesis by-products or environmental contaminants (i.e., leftover heavy metal catalysts or adsorption of PAHs) promoting genotoxic responses in cell systems incubated with carbon nanotubes [59]. Researchers are encouraged to expose cells to sample filtrates after nanomaterials have been removed from dosing solutions to ensure that the observed genotoxic response is due to the nanomaterials and not due to chemicals leached from the nanomaterials. Researchers are also encouraged to assess to what extent the presence of nanomaterials in test samples (as a consequence of incomplete nanomaterial removal before DNA damage analysis) influences the measured genotoxic response.
4. Other researchers have noted that nanomaterials can produce incorrect readouts in genotoxicity assays by physically or chemically interacting with assay components [171]. For accurate determinations of in vitro DNA damage, it is essential that the cells are viable before, during, and after the measurement. Nonviable cells (e.g., cells undergoing apoptosis) generate fragmented DNA and fragmented DNA is not an accurate reflection of the oxidative damage induced by the nanomaterial [12, 15].
5. For many metallic nanomaterials, it is important to assess the extent to which released ions account for the observed genotoxic response. This would help determine to what extent the observed DNA damage stems from the nanomaterials themselves or from released ions.
6. Relatively few in vivo nanomaterial toxicity studies have been conducted to date. Previous researchers have observed profoundly different toxic responses in nanomaterial mammalian cell studies compared with nanomaterial mammal studies [3, 172]. For nanomaterial genotoxicity research, it is especially important to perform in vivo studies in order to extrapolate the observed genotoxic responses to humans.
7. There is also a distinct lack of ecotoxicological research in this field. Only a handful of studies have explored the extent to which nanomaterials could induce oxidative damage to DNA in ecological receptors [125, 142, 144, 162, 163], yet these organisms are expected to be exposed to significant quantities of ENs in coming years.

Acknowledgements The authors would like to thank Miral Dizdaroglu (NIST) for carefully reviewing the manuscript during its preparation and Jerry Rattanong (Georgetown University) for editorial assistance.

Disclaimer Certain commercial equipment, instruments, and materials are identified to specify experimental procedures as completely as possible. In no case does such identification imply a recommendation or endorsement by the NIST nor does it imply that any of the materials, instruments, or equipment identified are necessarily the best available for the purpose.

References

1. Nel A, Xia T, Madler L, Li N (2006) Science 311:622–627
2. Li N, Xia T, Nel AE (2008) Free Radic Biol Med 44:1689–1699
3. Warheit DB (2008) Toxicol Sci 101:183–185
4. Gonzalez L, Lison D, Kirsch-Volders M (2009) Nanotoxicology 2:252–273
5. Schins RPF, van Berlo D, Wessels A, Gerloff K, Boots A, Scherbart A, Cassee FR, Gerlofs-Nijland M, Fokkens P, Schooten FJ, Albrecht C (2009) Mutagenesis 24:24

6. Singh N, Manshian B, Jenkins GJS, Griffiths SM, Williams PM, Maffeis TGG, Wright CJ, Doak SH (2009) Biomaterials 30:3891–3914
7. Halliwell B, Gutteridge JMC (2007) Free radicals in biology and medicine. Oxford University Press, New York
8. Knaapen AM, Seiler F, Schilderman PAEL, Nehls P, Bruch J, Schins RPF, Borm PJA (1999) Free Radic Biol Med 27:234–240
9. Evans DE, Dizdaroglu M, Cooke MS (2004) Mutat Res 567:1–61
10. Khanna KK, Jackson SP (2001) Nat Genet 27:247–254
11. Lan L, Nakajima S, Oohata Y, Takao M, Okano S, Masutani M, Wilson SH, Yasui A (2004) Proc Natl Acad Sci USA 101:13738–13743
12. Olive PL, Banath JP (2006) Nat Protoc 1:23–29
13. Collins AR (2004) Mol Biotechnol 26:249–261
14. Kumaravel TS, Vilhar B, Faux SP, Jha AN (2009) Cell Biol Toxicol 25:53–64
15. Tice RR, Agurell E, Anderson D, Burlinson B, Hartmann A, Kobayashi H, Miyamae Y, Rojas E, Ryu JC, Sasaki YF (2000) Environ Mol Mutagen 35:206–221
16. Johansson C, Moller P, Forchhammer L, Loft S, Godschalk RWL, Langie SAS, Lumeij S, Jones GDD, Kwok RWL, Azqueta A, Phillips DH, Sozeri O, Routledge MN, Charlton AJ, Riso P, Porrini M, Allione A, Matullo G, Palus J, Stepnik M, Collins AR, Moller L (2009) Mutagenesis 25:125–132
17. Forchhammer L, Brauner EV, Folkmann JK, Danielsen PH, Nielsen C, Jensen AW, Loft S, Friis G, Moller P (2008) Mutagenesis 23:223–231
18. Mroz RM, Schins RPF, Li H, Jimenez LA, Drost EM, Holownia A, MacNee W, Donaldson K (2008) Eur Respir J 31:241–251
19. Gurr JR, Wang ASS, Chen CH, Jan KY (2005) Toxicology 213:66–73
20. Jacobsen NR, Pojana G, White P, Moller P, Cohn CA, Korsholm KS, Vogel U, Marcomini A, Loft S, Wallin H (2008) Environ Mol Mutagen 49:476–487
21. Jacobsen NR, Saber AT, White P, Moller P, Pojana G, Vogel U, Loft S, Gingerich J, Soper L, Douglas GR, Wallin H (2007) Environ Mol Mutagen 48:451–461
22. Karlsson HL, Cronholm P, Gustafsson J, Moller L (2008) Chem Res Toxicol 21:1726–1732
23. Karlsson HL, Gustafsson J, Cronholm P, Moller L (2009) Toxicol Lett 188:112–118
24. Muslimovic A, Ismail IH, Gao Y, Hammarsten O (2008) Nat Protoc 3:1187–1193
25. Rogakou EP, Pilch DR, Orr AH, Ivanova VS, Bonner WM (1998) J Biol Chem 273:5858–5868
26. Shafirovich V, Singh C, Geacintov NE (2003) J Chem Educ 80:1297–1299
27. Olive PL (2006) Environ Mol Mutagen 11:487–495
28. Olive PL, Chan APS, Cu CS (1988) Cancer Res 48:6444–6449
29. Dizdaroglu M, Jaruga P, Birincioglu M, Rodriguez H (2002) Free Radic Biol Med 32:1102–1115
30. Voller A, Bartlett A, Bidwell DE (1978) J Clin Pathol 31:507–520
31. Burnett R, Guichard Y, Barale E (1997) Toxicology 119:83–93
32. Dorsey JG, Cooper WT (1994) Anal Chem 66:857A–867A
33. Greenberg MM, Hantosi Z, Wiederholt CJ, Rithner CD (2001) Biochemistry 40:15856–15861
34. Feig DI, Sowers L, Loeb LA (1994) Proc Natl Acad Sci USA 91:6609–6613
35. Kreutzer DA, Essigmann JM (1998) Proc Natl Acad Sci USA 95:3578–3582
36. Purmal AA, Kow TW, Wallace SS (1994) Nucleic Acids Res 22:3930–3935
37. Wallace SS (2002) Free Radic Biol Med 33:1–14
38. Delaney MO, Wiederholt CJ, Greenberg MM (2002) Angew Chem Int Ed 41:771–773
39. Wiederholt CJ, Greenberg MM (2002) J Am Chem Soc 124:7278–7279
40. Dizdaroglu M, Kirkali G, Jaruga P (2008) Free Radic Biol Med 45:1610–1621
41. Kalam MA, Haraguchi K, Chandani S, Loechler EL, Moriya M, Greenberg MM, Basu AK (2006) Nucleic Acids Res 34:2305–2315
42. Hurt RH, Monthioux M, Kane A (2006) Carbon 44:1028–1033
43. Landsiedel R, Kapp MD, Schulz M, Wiench K, Oesch F (2009) Mutat Res Rev Mutat Res 681:241–258
44. Gerloff K, Albrecht C, Boots AW, Forster I, Schins RPF (2009) Nanotoxicology 3:355–364
45. Mroz RM, Schins RPF, Li H, Drost EM, Macnee W, Donaldson K (2007) J Physiol Pharmacol 58:461–470
46. Yang H, Liu C, Yang DF, Zhang HS, Xi ZG (2009) J Appl Toxicol 29:69–78
47. Zhong BZ, Whong WZ, Ong TM (1997) Mutat Res Genet Toxicol Environ Mutagen 393:181–187
48. Jacobsen NR, Moller P, Jensen KA, Vogel U, Ladefoged O, Loft S, Wallin H (2009) Part Fibre Toxicol 6:2
49. Totsuka Y, Higuchi T, Imai T, Nishikawa A, Nohmi T, Kato T, Masuda S, Kinae N, Hiyoshi K, Ogo S, Kawanishi M, Yagi T, Ichinose T, Fukumori N, Watanabe M, Sugimura T, Wakabayashi K (2009) Part Fibre Toxicol 6:23
50. Gallagher J, Sams R, Inmon J, Gelein R, Elder A, Oberdorster G, Prahalad AK (2003) Toxicol Appl Pharmacol 190:224–231
51. Kisin ER, Murray AR, Keane MJ, Shi XC, Schwegler-Berry D, Gorelik O, Arepalli S, Castranova V, Wallace WE, Kagan VE, Shvedova AA (2007) J Toxicol Environ Health Part A 70:2071–2079
52. Lindberg HK, Falck GCM, Suhonen S, Vippola M, Vanhala E, Catalan J, Savolainen K, Norppa H (2009) Toxicol Lett 186:166–173
53. Pacurari M, Yin XJ, Ding M, Leonard SS, Schwegler-Berry D, Ducatman BS, Chirila M, Endo M, Castranova V, Vallyathan V (2008) Nanotoxicology 2:155–170
54. Pacurari M, Yin XJ, Zhao JS, Ding M, Leonard SS, Schwegler-Berry D, Ducatman BS, Sbarra D, Hoover MD, Castranova V, Vallyathan V (2008) Environ Health Perspect 116:1211–1217
55. Zeni O, Palumbo R, Bernini R, Zeni L, Sarti M, Scarfi MR (2008) Sensors 8:488–499
56. Zhu L, Chang DW, Dai LM, Hong YL (2007) Nano Lett 7:3592–3597
57. Poland CA, Duffin R, Kinloch I, Maynard A, Wallace WAH, Seaton A, Stone V, Brown S, MacNee W, Donaldson K (2008) Nat Nanotechnol 3:423–428
58. Shvedova AA, Kisin ER, Porter D, Schulte P, Kagan VE, Fadeel B, Castranova V (2009) Pharmacol Ther 121:192–204
59. Jakubek LM, Marangoudakis S, Raingo J, Liu XY, Lipscombe D, Hurt RH (2009) Biomaterials 30:6351–6357
60. Liu XY, Gurel V, Morris D, Murray DW, Zhitkovich A, Kane AB, Hurt RH (2007) Adv Mater 19:2790
61. Folkmann JK, Risom L, Jacobsen NR, Wallin H, Loft S, Moller P (2009) Environ Health Perspect 117:703–708
62. Cherukuri P, Gannon CJ, Leeuw TK, Schmidt HK, Smalley RE, Curley SA, Weisman B (2006) Proc Natl Acad Sci USA 103:18882–18886
63. Liu Z, Davis C, Cai WB, He L, Chen XY, Dai HJ (2008) Proc Natl Acad Sci USA 105:1410–1415
64. Singh R, Pantarotto D, Lacerda L, Pastorin G, Klumpp C, Prato M, Bianco A, Kostarelos K (2006) Proc Natl Acad Sci USA 103:3357–3362
65. Yang ST, Guo W, Lin Y, Deng XY, Wang HF, Sun HF, Liu YF, Wang X, Wang W, Chen M, Huang YP, Sun YP (2007) J Phys Chem C 111:17761–17764

66. Ferguson PL, Chandler GT, Templeton RC, Demarco A, Scrivens WA, Englehart BA (2008) Environ Sci Technol 42:3879–3885
67. Leeuw TK, Reith RM, Simonette RA, Harden ME, Cherukuri P, Tsyboulski DA, Beckingham KM, Weisman RB (2007) Nano Lett 7:2650–2654
68. Petersen EJ, Akkanen J, Kukkonen JVK, Weber WJ Jr (2009) Environ Sci Technol 43:2969–2975
69. Petersen EJ, Huang QG, Weber WJ Jr (2010) Environ Toxicol Chem 29:1106–1112
70. Petersen EJ, Huang QG, Weber WJ Jr (2008) Environ Sci Technol 42:3090–3095
71. Petersen EJ, Huang QG, Weber WJ Jr (2008) Environ Health Perspect 116:496–500
72. Worle-Knirsch JM, Pulskamp K, Krug HF (2006) Nano Lett 6:1261–1268
73. Lin MH, Hsu TS, Yang PM, Tsai MY, Perng TP, Lin LY (2009) Int J Radiat Biol 85:214–226
74. Brown DM, Kinloch IA, Bangert U, Windle AH, Walter DM, Walker GS, Scotchford CA, Donaldson K, Stone V (2007) Carbon 45:1743–1756
75. Dhawan A, Taurozzi JS, Pandey AK, Shan WQ, Miller SM, Hashsham SA, Tarabara VV (2006) Environ Sci Technol 40:7394–7401
76. Jafvert CT, Kulkarni PP (2008) Environ Sci Technol 42:5945–5950
77. Henry TB, Menn FM, Fleming JT, Wilgus J, Compton RN, Sayler GS (2007) Environ Health Perspect 115:1059–1065
78. Kovochich M, Espinasse B, Auffan M, Hotze EM, Wessel L, Xia T, Nel AE, Wiesner MR (2009) Environ Sci Technol 43:6378–6384
79. Spohn P, Hirsch C, Hasler F, Bruinink A, Krug HF, Wick P (2009) Environ Pollut 157:1134–1139
80. Bernstein R, Prat F, Foote CS (1999) J Am Chem Soc 121:464–465
81. Isakovic A, Markovic Z, Todorovic-Markovic B, Nikolic N, Vranjes-Djuric S, Mirkovic M, Dramicanin M, Harhaji L, Raicevic N, Nikolic Z, Trajkovic V (2006) Toxicol Sci 91:173–183
82. Sera N, Tokiwa H, Miyata N (1996) Carcinogenesis 17:2163–2169
83. Tokuyama H, Yamago S, Nakamura E (1993) J Am Chem Soc 115:7918–919
84. Nielsen GD, Roursgaard M, Jensen KA, Poulsen SS, Larsen ST (2008) Basic Clin Pharmacol Toxicol 103:197–208
85. Moreira S, Silva NB, Almeida-Lima J, Rocha HAO, Medeiros SRB, Alves C, Gama FM (2009) Toxicol Lett 189:235–241
86. Colognato R, Bonelli A, Ponti J, Farina M, Bergamaschi E, Sabbioni E, Migliore L (2008) Mutagenesis 23:377–382
87. Ponti J, Sabbioni E, Munaro B, Broggi F, Marmorato P, Franchini F, Colognato R, Rossi F (2009) Mutagenesis 24:439–445
88. Colvin VL (2003) Nat Biotechnol 21:1166–1170
89. Oberdorster G, Oberdorster E, Oberdorster J (2005) Environ Health Perspect 113:823–839
90. Papageorgiou I, Brown C, Schins R, Singh S, Newson R, Davis S, Fisher J, Ingham E, Case CP (2007) Biomaterials 28:2946–2958
91. Bhabra G, Sood A, Fisher B, Cartwright L, Saunders M, Evans WH, Surprenant A, Lopez-Castejon G, Mann S, Davis SA, Hails LA, Ingham E, Verkade P, Lane J, Heesom K, Newson R, Case CP (2009) Nat Nanotechnol 4:876–883, http://www.nature.com/nnano/journal/v4/n12/pdf/nnano.2009.313.pdf
92. Baldwin EL, Byl JA, Osheroff N (2004) Biochemistry 43:728–735
93. Kopera E, Schwerdtle T, Hartwig A, Bal W (2004) Chem Res Toxicol 17:1452–1458
94. Midander M, Cronholm P, Karlsson HL, Elihn K, Moller L, Leygraf C, Wallinder IO (2009) Small 5:389–399
95. Connor EE, Mwamuka J, Gole A, Murphy CJ, Wyatt MD (2005) Small 1:325–327
96. Ponti J, Colognato R, Franchini F, Gioria S, Simonelli F, Abbas K, Uboldi C, Kirkpatrick CJ, Holzwarth U, Rossi F (2009) Nanotoxicology 3:296–306
97. Rosi NL, Giljohann DA, Thaxton CS, Lytton-Jean AKR, Han MS, Mirkin CA (2006) Science 312:1027–1030
98. Shenoy D, Fu W, Li JB, Crasto C, Jones G, DimMarzio C, Sridhar S, Amiji M (2006) J Nanomed 1:51–57
99. Shukla R, Bansal V, Chaudhary M, Basu A, Bhonde RR, Sastry M (2005) Langmuir 21:10644–10654
100. Tkachenko AG, Xie H, Liu T, Coleman D, Ryan J, Glomm W, Shipton MK, Franzen S, Feldheim DL (2004) Bioconjug Chem 14:482–490
101. Tsoli M, Kuhn H, Brandau W, Esche H, Schmid G (2005) Small 1:841–844
102. Kang B, Mackey MA, El-Sayed MA (2010) J Am Chem Soc 132:1517–1519
103. Grigg J, Tellabati A, Rhead S, Almeida GM, Higgins JA, Bowman KJ, Jones GD, Howes PB (2009) Nanotoxicology 3:348–345
104. Kang JS, Yum YN, Kim JH, Song H, Jeong J, Lim YT, Chung BH, Park SN (2009) Biomol Ther 17:92–97
105. Li JJ, Zou L, Hartono D, Ong CN, Bay BH, Yung LYL (2008) Adv Mater 20:138–142
106. Chithrani BD, Ghazani AA, Chan WCW (2006) Nano Lett 6:662–668
107. Chithrani BD, Chan WCW (2007) Nano Lett 7:1542–1550
108. Zhang Q, Kusaka Y, Sato K (1998) J Toxicol Environ Health Part A 53:423–438
109. Pelka J, Gehrke H, Esselen M, Turk M, Crone M, Brase S, Muller T, Blank H, Send W, Zibat V, Brenner P, Schneider R, Gerthsen D, Marko D (2009) Chem Res Toxicol 22:649–659
110. Coste F, Ober M, Carell T, Boiteux S, Zelwer C, Castaing B (2004) J Biol Chem 279:44074–44083
111. Navarro E, Piccapietra F, Wagner B, Marconi F, Kaegi R, Odzak N, Sigg L, Behra R (2008) Environ Sci Technol 42:8959–8964
112. Arakawa H, Neault JF, Tajmir-Riahi HA (2001) Biophys J 81:1580–1587
113. Ahamed M, Karns M, Goodson M, Rowe J, Hussain SM, Schlager JJ, Hong YL (2008) Toxicol Appl Pharmacol 233:404–410
114. AshaRani PV, Mun GLK, Hande MP, Valiyaveettil S (2009) ACS Nano 3:279–290
115. Kim S, Choi JE, Choi J, Chung KH, Park K, Yi J, Ryu DY (2009) Toxicol In Vitro 23:1076–1084
116. Sawosz E, Grodzik M, Zielinska M, Niemiec T, Olszanka B, Chwalibog A (2009) Arch Geflugelk 73:208–213
117. Aruoma OI, Halliwell B, Gajewski E, Dizdaroglu M (1989) J Biol Chem 264:20509–20512
118. Aruoma OI, Halliwell B, Gajewski E, Dizdaroglu M (1991) Biochem J 273:601–604
119. Gwinn MR, Leonard SS, Sargent LM, Lowry DT, McKinstry KT, Meighan T, Reynolds SH, Kashon M, Castranova V, Vallyathan V (2009) J Toxicol Environ Health Part A 72:1509–1519
120. Chen M, von Mikecz A (2005) Exp Cell Res 305:51–62
121. Limbach LK, Wick P, Manser P, Grass RN, Bruinink A, Start WJ (2007) Environ Sci Technol 41:4158–4163
122. Barnes CA, Elsaesser A, Arkusz J, Smok A, Palus J, Lesniak A, Salvati A, Hanrahan JP, de Jong WH, Dziubaltowska E, Stepnik M, Rydzynski K, McKerr G, Lynch I, Dawson KA, Howard CV (2008) Nano Lett 8:3069–3074
123. Jin YH, Kannan S, Wu M, Zhao JXJ (2007) Chem Res Toxicol 20:1126–1133
124. Wang JJ, Sanderson BJS, Wang H (2007) Environ Mol Mutagen 48:151–157

125. Lee SW, Kim SM, Choi J (2009) Environ Toxicol Pharmacol 28:86–91
126. Kim YJ, Choi HS, Song MK, Youk DY, Kim JH, Ryu JC (2009) Molecul Cell Toxicol 5:172–178
127. Balasubramanyam A, Sailaja N, Mahboob M, Rahman MF, Hussain SM, Grover P (2009) Mutagenesis 24:245–251
128. Pierscionek BK, Li YB, Yasseen AA, Colhoun LM, Schachar RA, Chen W (2010) Nanotechnology 21:035102
129. Rothen-Rutishauser B, Grass RN, Blank F, Limbach LK, Muehlfeld C, Brandenberger C, Raemy DO, Gehr P, Stark WJ (2009) Environ Sci Technol 43:2634–2640
130. Auffan M, Rose J, Orsiere T, Meo MD, Thill A, Zeyons O, Proux O, Masion A, Chaurand P, Spalla O, Botta A, Wiesner MR, Bottero JY (2009) Nanotoxicology 3:161–171
131. Stone V, Johnston H, Schins RPF (2009) Crit Rev Toxicol 39:613–626
132. Fahmy B, Cormier SA (2009) Toxicol In Vitro 23:1365–1371
133. Auffan M, Decome L, Rose J, Orsiere T, De Meo M, Briois V, Chaneac C, Olivi L, Berge-Lefranc JL, Botta A, Wiesner MR, Bottero JY (2006) Environ Sci Technol 40:4367–4373
134. Bhattacharya K, Davoren M, Boertz J, Schins RPF, Hoffmann E, Dopp E (2009) Part Fibre Toxicol 6:17
135. Petrat F, Paluch S, Dogruoz E, Dorfler P, Kirsch M, Korth HG (2003) J Biol Chem 278:46403–46413
136. Dunford R, Salinaro A, Cai L, Serpone N, Horikoshi S, Hidaka H, Knowland J (1997) FEBS Lett 418:87–90
137. Gottschalk F, Sonderer T, Scholz RW, Nowack B (2009) Environ Sci Technol 43:9216–9222
138. Mueller NC, Nowack B (2008) Environ Sci Technol 42:4447–4453
139. Hirakawa K, Mori M, Yoshida M, Oikawa S, Kawanishi S (2004) Free Radic Res 38:439–447
140. Kemp TJ, McIntyre RA (2007) Prog React Kinet Mech 32:219–229
141. Nakagawa Y, Wakuri S, Sakamoto K, Tanaka K (1997) Mutat Res 394:125–132
142. Reeves JF, Davies SJ, Dodd NJF, Jha AN (2008) Mutat Res 640:113–122
143. Serpone N, Salinaro AE, Horikoshi S, Hidaka H (2006) J Photochem Photobiol A 179:200–212
144. Vevers WF, Jha AN (2008) Ecotoxicology 17:410–420
145. Zhu RR, Wang SL, Chao J, Shi DL, Zhang R, Sun XY, Yao SD (2009) Mater Sci Eng C 29:691–696
146. Gopalan RC, Osman IF, Amani A, Matas MD, Anderson D (2009) Nanotoxicology 3:33–39
147. Huang NP, Xu MH, Yuan CW, Yu RR (1997) J Photochem Photobiol A 108:229–233
148. Falck GCM, Lindberg HK, Suhonen S, Vippola M, Vanhala E, Catalan J, Savolainen K, Norppa H (2009) Hum Exp Toxicol 28:339–352
149. Kang SJ, Kim BM, Lee YJ, Chung HW (2008) Environ Mol Mutagen 49:399–405
150. Wang JJ, Sanderson BJS, Wang H (2007) Mutat Res Genet Toxicol Environ Mutagen 628:99–106
151. Sato T, Taya M (2006) Biochem Eng J 28:303–308
152. Dodd NJF, Jha AN (2009) Mutat Res Fundam Molecul Mech Mutagen 660:79–82
153. Rehn B, Seiler F, Rehn S, Bruch J, Maier M (2003) Toxicol Appl Pharmacol 189:84–95
154. Trouiller B, Reliene R, Westbrook A, Solaimani P, Schiestl RH (2009) Cancer Res 69:8784–8789
155. Lin WS, Xu Y, Huang CC, Ma YF, Shannon KB, Chen DR, Huang YW (2009) J Nanopart Res 11:25–39
156. Sharma V, Shukla RK, Saxena N, Parmar D, Das M, Dhawan A (2009) Toxicol Lett 185:211–218
157. Mahendra S, Zhu HG, Colvin VL, Alvarez PJ (2008) Environ Sci Technol 42:9424–9430
158. Green M, Howman E (2005) Chem Commun 121–123
159. Hoshino A, Fujioka K, Oku T, Suga M, Sasaki YF, Ohta T, Yasuhara M, Suzuki K, Yamamoto K (2004) Nano Lett 4:2163–2169
160. Anas A, Akita H, Harashima H, Itoh T, Ishikawa M, Biju V (2008) J Phys Chem B 112:10005–10011
161. Mottley C, Harman LS, Mason RP (1985) Biochem Pharmacol 34:3005–3008
162. Gagne F, Auclair J, Turcotte P, Fournier M, Gagnon C, Sauve S, Blaise C (2008) Aquat Toxicol 86:333–340
163. Gagne F, Maysinger D, Andre C, Blaise C (2008) Nanotoxicology 2:113–120
164. Badisa VLD, Latinwo LM, Odewumi CO, Ikediobi CO, Badisa RB, Ayuk-Takem LT, Nwoga J, West J (2007) Environ Toxicol 22:144–151
165. Faverney CR, Devaux A, Lafaurie M, Girard JP, Bailly B, Rahmani R (2001) Aquat Toxicol 53:65–76
166. Hossain Z, Huq F (2002) J Inorg Biochem 90:85–96
167. Prakash AS, Rao KS, Dameron CT (1998) Biochem Biophys Res Commun 244:198–203
168. Dizdaroglu M (1998) Free Radic Res 29:551–563
169. ESCODD (2003) Free Radic Biol Med 34:1089–1099
170. Park H, Grassian VH (2010) Environ Toxicol Chem 29:715–721
171. Doak SH, Griffiths SM, Manshian B, Singh N, Williams PM, Brown AP, Jenkins GJS (2009) Mutagenesis 24:285–293
172. Sayes CM, Marchione AA, Reed KL, Warheit DB (2007) Nano Lett 7:2399–2406
173. Rakiman I, Chinnadurai M, Baraneedharan U, Paul SFD, Venkatachalam P (2008) Adv Biotechnol 7:39–41